PAPER

Hydrogeological origin of the CO_2-rich mineral water of Vilajuïga in the Eastern Pyrenees (NE Catalonia, Spain)

Josep Mas-Pla[1,2] · David Brusi[1] · Carles Roqué[1] · David Soler[1] · Anna Menció[1] · Josep M Costa[1] · Manuel Zamorano[1] · Warren Meredith[1]

Abstract

The mineral water of Vilajuïga village in Alt Empordà (NE Catalonia, Spain) owes its uniqueness to an emanation of geogenic CO_2 that modifies groundwater hydrochemistry to produce a differentiated HCO_3–Na- and CO_2-rich groundwater among the usual Ca–HCO_3 type found in this region. A hydrogeological conceptual model attributes its occurrence to the intersection of two faults: La Valleta and Garriguella-Roses. The former provides a thrust of metamorphic over igneous rocks, formed during the Paleozoic, over a layer of ampelitic shale that, from a hydrogeological perspective, acts as a confining layer. The Garriguella-Roses normal fault, which originated during the Neogene, permits the degassing of geogenic CO_2 that is attributed to volcanic activity occurring in the Neogene. Groundwater mixing from the metamorphic and igneous rock units plus the local occurrence of CO_2 creates a HCO_3–Na water that still holds free-CO_2 in solution. Interaction with the gas phase is restricted at the intersection of the two faults. Radiocarbon dating, after correcting for geogenic dead carbon, estimates an age of 8,000 years BP. The low tritium content (0.7 TU) indicates that Vilajuïga water is a mix of "older" groundwater recharged in the metamorphic rocks of the Albera range and "younger" groundwater from the igneous rocks of the Rodes range, over a recharge area of 45 km^2 and a maximum elevation of 600 m. Given its origin as rare groundwater in the southern slope of the Eastern Pyrenees, purposeful monitoring is necessary to evaluate the groundwater vulnerability and anticipate impacts from nearby wells and climate-change effects.

Keywords Fault hydrogeology · Hydrochemistry · Fluid–rock interaction · Groundwater age · Stable isotopes

Introduction

Groundwater springs have traditionally been places of interest, whether for bathing or drinking, based on the assumed therapeutic benefits supported by their richness in rare, unusual or even radioactive properties. Most of them have undergone economic consideration in terms of bottled water for drinking, medicinal use or mineral exploitation, or they have been developed as spas throughout history (LaMoreaux and Tanner 2001). The terms "mineral water" or "mineral spring water" can be widely defined as a source for water which has one or more chemical characteristics different from normal potable water used for public use (Kresic and Stevanovic 2010). Indeed, the chemical composition of spring waters reflects the interaction of groundwater with the aquifer host rock as well as with any other chemical component, including gases such as carbon dioxide, and in some places the effect of temperature which, in the end, controls all geochemical processes.

From a hydrogeological perspective, the occurrence of singular springs provides an opportunity to unveil the hydrogeological processes that, firstly, determine their discharge at that specific location and, secondly, identify the hydrochemical origin of its composition (Tweed et al. 2004). Such effort usually relies on previous knowledge of the geological setting that determines the local outcropping conditions; however, it is also common to use the chemistry of the mineral spring water to decipher groundwater flow paths, unobserved water–rock interactions, and mixing of water from

✉ Josep Mas-Pla
josep.mas@udg.edu

1 Grup de Geologia Aplicada i Ambiental (GAiA), Centre de Recerca en Geologia i Cartografia Ambiental (Geocamb), Dept. de Ciències Ambientals, Universitat de Girona, 17003 Girona, Spain

2 Institut Català de Recerca de l'Aigua (ICRA), 17003 Girona, Spain

distinct recharge areas. Numerous case studies of spring waters around the world (e.g., Pauwels et al. 1997; Cerón et al. 2000; Marqués et al. 2001; Cartwright et al. 2002; Carreira et al. 2014) are considered as examples to describe the specificities of groundwater flow under particular conditions, usually in complex tectonic environments, or to test the goodness of particular hydrogeochemical approaches to reveal the governing hydrogeological processes in detail. Moreover, both location and specific water quality have presently acquired historical relevance and assigned a heritage value to these springs (e.g., Gray 2013)

The Vilajuïga mineral water is one of these special examples of "distinct" water with an actual heritage value due to its chemical composition. It is a sodium-rich bicarbonate water, with a sparkling taste derived from its high partial pressure of carbon dioxide at the surface, and noticeable concentrations of lithium, as promoted by early medical advertisements. Originally, this water occurred in a few shallow wells in the small municipality of Vilajuïga (Alt Empordà, NE Catalonia, Spain; Fig. 1). In 1902, after a chemical analysis that defined its chemical composition and described its medicinal properties, the discharge obtained from a shallow exploitation well was commercialized and continues to be so at present through deeper wells with the same hydrochemical characteristics. Its unique discharge location with no other currently existing source, spring or well nearby with a similar chemical composition, represents a puzzling occurrence that, despite being geologically studied just after its unearthing (Font i Sagué, Memoria y descripción geológica de las aguas líticas de Vilajuïga [Memoir and geological description of the lithic waters of Vilajuïga]. Report funded by the Society "Martí Badosa i Cía", unpublished, 1909), has not further been considered in hydrogeological literature. In this sense, the source of the Vilajuïga mineral water provides an opportunity to explore the influences of geology and tectonics in the groundwater flow and, correspondingly, to determine such influences using geochemical and isotopic tools, including the effect of geogenic produced carbon dioxide.

Groundwater flow in these spring systems is usually driven by faults, which is the reason for their movement upwards and their outcropping at the surface (e.g., Bense et al. 2013; Folch and Mas-Pla 2008). Vilajuïga is located on the main distensive fault line (the Garriguella-Roses fault) that separates the Empordà basin from the most eastward part of the Pyrenees Axial zone (Fig. 1). Moreover, its location coincides with an intersection of this fault with an ancient thrust (La Valleta Fault) affecting the rocks of the Axial zone. This study addresses the potential role of both tectonic structures in the regional flow field, the combined hydrogeological behavior of the diverse metamorphic and igneous rocks of the Pyrenees, and the sedimentary infilling

of the Empordà basin, as well as the reasons why a CO_2-rich mineral water appears at this specific geological setting.

The aim of this study is to describe the singular hydrogeological system of the Vilajuïga CO_2-rich mineral water, using hydrogeological and hydrochemical information to discern the groundwater flow path. Since the hydrogeological case of the Vilajuïga mineral water is unique in this region, such knowledge of its functioning can contribute to a better understanding of similar hydrogeological environments and their protection (Carreira et al. 2014; Choi et al. 2014; Do et al. 2020; Evans et al. 2002; Schofield and Jankowski 2004). Therefore, determining the processes that control their occurrence and quality is essential for effective management and protection of a water resource (Foster and Garduño 2012), specifically in an area where the physical hydrogeology is complex and pressures from other groundwater uses, and even climate change, can eventually alter its hydrochemical composition and affect its exploitation rate and its heritage value.

Brief history of the Vilajuïga mineral water

As explained by Masanés (2021), the Vilajuïga water was known from ancient times, yet the first documents regarding its occurrence in a few shallow wells within the municipality date from the 19th century. By 1902, a private owner began the exploitation of the well Margineda and, after the analyses that defined its composition and therapeutic properties, the mineral water was legally accepted for public use and commercialization. A new open well was drilled in 1909—Well Escaire; Fig. SM1 in the electronic supplementary material (ESM)—to supply the demand. The Vilajuïga water became popular and the village developed a tourist sector from the early 1920s until the Spanish Civil War (1936–1939). Despite the poverty and the change of social habits that followed the war, the exploitation of the Vilajuïga water continued. In fact, its popularity increased along with its production, and even the surrealist painter Salvador Dalí, who was born in the nearby town of Figueres, was a usual consumer of Vilajuïga water. Daily production increased by 1980 and a second well (well Nou) was drilled to meet such a large demand.

The arrival of international brands to the bottled water market had an impact on small producers, and the Vilajuïga water firm had to close in 2009. However, Group Grifols, a global pharmaceutical company settled in Barcelona (Spain) and, concerned about the heritage value of this mineral water, took over the business in 2017. The company drilled a new borehole (well Grifols), modernized the bottling plant, and brought the water back to the market. Currently, wells Escaire and Grifols are the only sources of Vilajuïga water, both with identical chemical composition, with the latter dedicated to production (Fig. SM1 in the ESM).

General geological setting

Vilajuïga and the complete study area lie on the geological contact between the Pyrenees and the Empordà basin. The Empordà basin is a tectonic graben defined by a NW–SE-trending fault system, surrounded by the Pyrenees Axial zone in the north, the South Pyrenean Zone and the Transverse Range in the west, and the Gavarres Range in the south (e.g., Pujadas et al. 1989; Saula et al. 1996). Its origin is associated to the Mediterranean Sea development during the Neogene (e.g., Lewis et al. 2000). The geologic framework for the study area (Soler et al. 2014; Fig. 1) is as follows:

1. The *Pyrenees Axial zone* formed in its easternmost area by the Albera and Rodes ranges with their extension to Cap de Creus consisting of Paleozoic igneous and metamorphic rocks, affected by Variscan and Alpine orogenesis. In particular, the Axial zone is affected by diverse tectonic elements (faults, thrusts) that provide preferential groundwater flow paths.
2. The *Pre-Pyrenean Zone and Transversal Range* are mainly composed of Paleogene sedimentary rocks, but also of some Mesozoic deposits linked to thrust-fault structures. None of these units are in the study area.
3. The *Empordà basin* was developed during the Neogene as a graben structure limited by normal faults, which act as boundaries with the surrounding geological units. The following geological formations of interest are distinguished within the Empordà basin:

    - The Neogene deposits appear in areas close to ranges foothills and in the basin basement. They include a wide range of sedimentary environments from alluvial fans in the inland areas to marine facies near the coast (Fleta et al. 1991). Within these formations, aquifers are laterally discontinuous, and located in the coarser materials (mainly gravels and sands). They constitute the southern limit of the study area.
    - The Quaternary fluvio-deltaic formations are related to the recent evolution (late Pleistocene-Holocene) of the Muga, Fluvià and Ter Rivers. These formations were developed due to recent eustatic changes and cover all the previous units with an unconformity contact. In this area, Quaternary formations present unconfined aquifers as well as leaky aquifers in the lowest strata (Bach 1986; Mas-Pla et al. 1999a, b; Montaner 2010). Even though not included in the study area, the fluvio-deltaic deposits of the Muga River receive groundwater discharge of the regional hydrogeological system that includes the Vilajuïga mineral water.
    - A thin layer of Quaternary alluvium and colluvium, with a maximum thickness of 10–15 m is devel-

oped at the foothills of Albera and Rodes ranges, specifically in the Vilajuïga area, and covers the hanging wall block of the northernmost fault that defines the Empordà basin.

As mentioned before, the tectonic structure of the Empordà basin graben is defined by a set of fault zones (Fig. 1). The most northern one, named the Garriguella-Roses fault, is the one linked to the Vilajuïga water source. Nevertheless, the hanging block wall of this fault is only covered by the Quaternary alluvium and colluvium that lay upon the igneous and metamorphic rocks of the Pyrenees. The Neogene basin begins at the block located SW of the Delfià-Marzà fault, where the sedimentary formation crops out. In the northern part of the Empordà basin, the maximum thickness of the Neogene deposits reaches near 2 km between the Sant Climent and La Jonquera faults (Fig. 1). Specifically, the geology of the main study area covers the southern slope of the Pyrenees Axial zone, formed by the Albera and Rodes ranges including the Quaternary deposits formed at the foothills, and ends at the limit set by the Delfià-Marzà fault. Since both regional faults are potentially related to the overall flow system, samples from springs and deep wells (60–80 m depth approx.) located in the vicinity of the Sant Climent and La Jonquera faults are also included in the study for reference. Moreover, since the groundwater natural discharge to the Mediterranean Sea takes place through the fluvio-deltaic formation of the Muga River, data from three wells located on its lower layers are also incorporated into the dataset of the study area.

Another tectonic element of relevance is a thrust fault, called La Valleta fault (Fig. 1), that displaced the metamorphic rocks of the Albera range over the igneous and metamorphic rocks of the Rodes range during the Variscan orogeny (late Paleozoic). Vilajuïga is located upon the intersection of this thrust line and the Garriguella-Roses fault, indicating that the occurrence of the CO_2-rich Vilajuïga water at this location may be related to the crossing of both structures.

Previous studies

No previous references exist on the hydrogeological system that produce Vilajuïga mineral water. Font i Sagué (Memoria y descripción geológica de las aguas líticas de Vilajuïga [Memoir and geological description of the lithic waters of Vilajuïga]. Report funded by the Society "Martí Badosa i Cía", unpublished, 1909) wrote the first description of the geology at the vicinity of the source, indicating that it discharges in the contact between igneous and metamorphic rocks (La Valleta fault) near a major normal fault (Garriguella-Roses fault) and identified the role of both
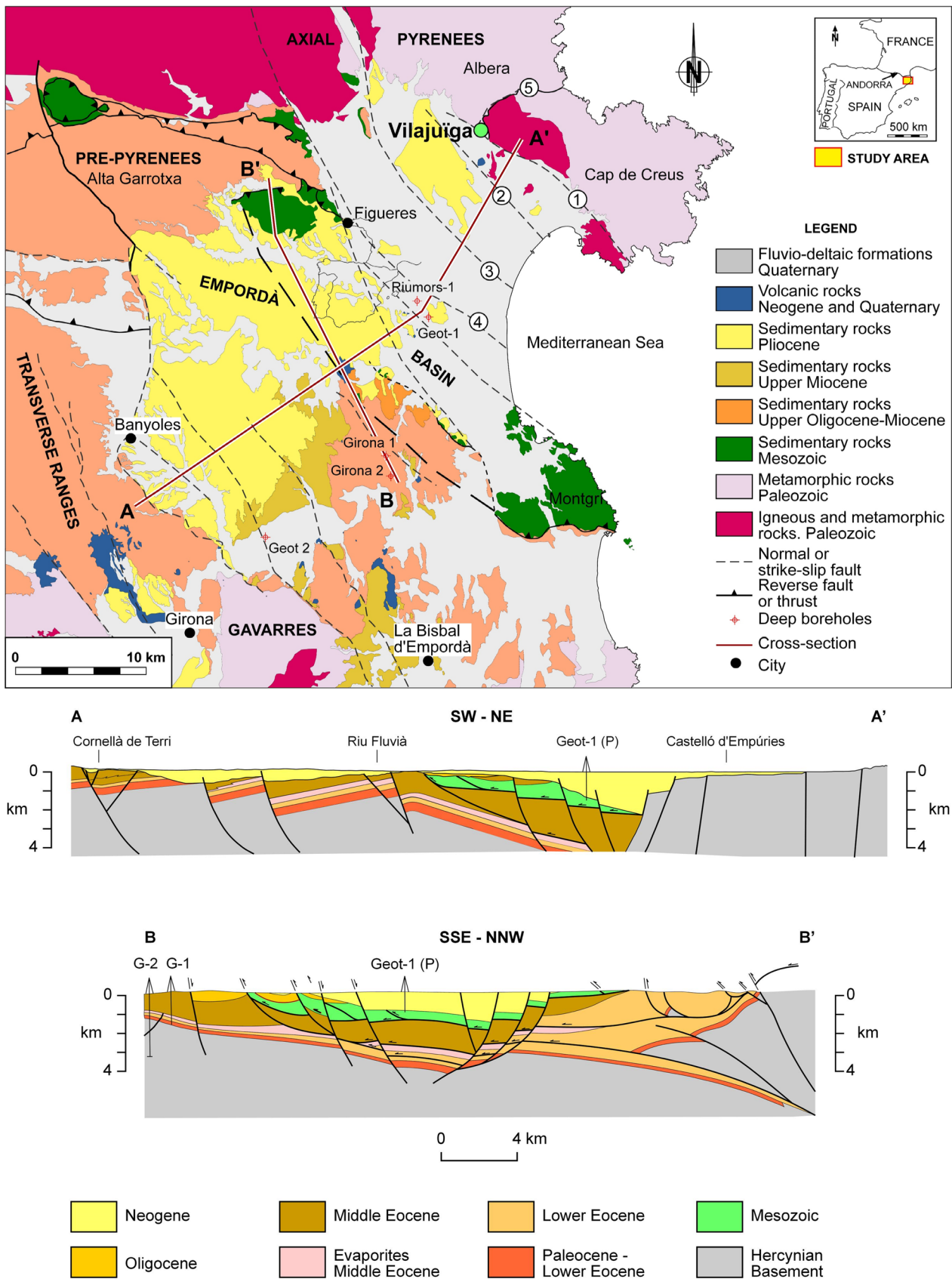
Fig. 1 Regional geological setting of the Vilajuïga area in the context of the Eastern Pyrenees and the Empordà basin. Identified fault names: 1 Garriguella-Roses; 2 Delfià-Marzà; 3 Sant Climent; 4 La Jonquera; 5 La Valleta. Modified after ICGC (2022)

regional fractures in the groundwater flow towards the surface. This work also acknowledged a layer of ampelitic black shale as a confining layer and recognized its effect on the local occurrence of the spring. Moreover, the work attributed the high CO_2 content as being of volcanic origin given the outcrop of volcanic rocks in nearby areas and the regional tectonic setting.

No other scientific reports had been published until the 1990's, when the bottling company commissioned hydrogeological studies to support the drilling of new wells. Among the most relevant, Geoconsulting (Estudios geológicos. Análisis bacteriológicos/Físico-Químicos [Geological studies: bacteriological/physical-chemical analysis]. Aigües de Vilajuïga, unpublished, 1994) provides a detailed geological map of the area and the borehole characteristics of well Nou (60 m depth) drilled in mainly granite rocks. In its shallow parts, the borehole penetrates the ampelitic shale (3–6 m thick) overlying a strained and fractured granodiorite with veins of diorite all along the borehole depth. Another report of relevance relates to the drilling of well Grifols (121 m depth; Oficina Técnica Minera, Estudi hidroquímic de la nova captació d'Aigües de Vilajuïga per a l'ampliació del reconeixement com a aigua mineral natural [Hydrochemical study of the new Aigües de Vilajuïga well for the extension of recognition as natural mineral water], unpublished, 2018). Its well log is similar to well Nou (the wells are within 50 m of each other), yet the ampelitic shale has a larger apparent thickness (30 m). The rest of the borehole was drilled in granitoid (probably granodiorite; 30–80 m depth) and granitoid with mafic minerals (probably granodiorite with diorite xenoliths; 80–121 m depth). The most productive part is between 40 and 80 m depth, and its resources have identical chemical composition to those of the previous wells, indicating that, despite lithological differences in the borehole record attributed to local tectonic details, all of them exploit the same groundwater system.

Methodology

Regional information was obtained from 1:25,000 geological maps (ICGC 2001, 2013), refined by field observations, and summarized to identify the main lithologies that control the groundwater geochemistry. Cross-sections were drawn according to field data.

Four electrical resistivity tomography (ERT) profiles were conducted in the surroundings of the source location to define the subsurface structure in its vicinity, and to establish the position of the main faults and the type of materials in each block. Measurements were carried out with a multi-electrode ABEM Terrameter LS2 by Guideline Geo, connected to 4 multicore cable reels linked in series, which in turn were nailed to the ground with evenly spaced stainless steel electrodes (0.5 m ERT-01; 1 m ERT-02; 10 m ERT-03; and 3 m ERT-04). Apparent resistivity data acquisition was conducted using the non-conventional multiple gradient array electrode configuration (Dahlin and Zhou 2006). The gradient array increases speed of data acquisition in the field and provides higher-density datasets compared to other conventional protocols. Length of ERT profiles ranged between 42 and 710 m, and the maximum depth of investigation was 7–120 m, respectively. Commercial Res2DInv package (Geotomo Software) was used for data processing and representation (Loke and Barker 1996). Iterative least squares inversion and finite-element forward modelling provided the final two-dimensional (2D) resistivity sections, which have low values of bulk root mean square error (RMS = 1.1–5.1%).

A sampling campaign, including 15 wells and 2 springs, was performed in November and December 2021 (Fig. SM2 in the ESM). Data were also used from seven additional groundwater samples from the Albera range and its fault zones (3 wells and 1 spring) and from the deeper layers of the Muga fluvio-deltaic deposits (3 wells), representing potential recharge and discharge areas, respectively, of the hydrogeological system that includes the Vilajuïga water (Soler et al. 2014; Mas-Pla et al. 2016a). Well depths are usually larger than 40 m, and most of them reach 100–120 m from the surface (refer to Table SM1 in the ESM), with the exception of well GAR05 (460 m depth).

Physico-chemical parameters (pH, Eh, electrical conductivity (EC), dissolved oxygen (DO), and temperature) were measured in situ with a flow cell to avoid contact with the atmosphere. Samples were stored at 4 °C in a dark environment for subsequent analyses of the hydrochemical parameters in the laboratory. Hydrochemical and isotope data were analysed by external laboratories using certified standard methods (Laboratori Dr. Oliver Rodés; SIDI-Universidad Autónoma de Madrid; Servei de Datació per Triti, Universitat Autònoma de Barcelona; Beta Analytic, Inc.). Isotopic data ($\delta^{18}O$ and δD) of water samples are expressed in terms of the per mille deviation of the isotope ratio of the sample relative to that of the V-SMOW standard. $\delta^{13}C$ data are also expressed in terms of per mille deviation of the isotope ratio of the sample relative to VPDB standard. Radiocarbon results were obtained on the dissolved inorganic carbon (DIC) and are reported as percent modern carbon (pMC). CO_2 partial pressure and saturation indices were calculated using PHREEQC (Parkhurst and Appelo 2013). The entire hydrochemical and isotopic dataset is provided as ESM.

Results

Main hydrogeological units: lithologies and structural features

Based on the geological maps from ICGC (2001, 2013; redrawn in Fig. 2), the hydrogeological units related to the hydrogeological system associated to the Vilajuïga water are as follows:

– *Hydrogeological unit in metamorphic rocks*. Mainly located in the Albera range and in the northern slope of the Rodes range. At the Albera range, west of La Valleta fault, the metamorphic sequence is dominated by Cambro-Ordovician and/or Neoproterorozoic greywackes, pelites and arenites with small intercalations of calcareous and volcanic rocks. Metasedimentary lithologies (schists, shales and marbles) are fairly uniform throughout the whole region. The metasedimentary sequence preserves a continuous low-pressure, high-temperature prograde metamorphism from SE to NW. From low to high metamorphic grade, the chlorite-muscovite, biotite, andalusite-cordierite, sillimanite and migmatite zones can be progressively distinguished (Vilà et al. 2007). At the Rodes range, east of La Valleta fault, the sequence of metasedimentary rocks is interrupted by leucocratic pegmatites in the form of dykes or irregular masses with dimensions to tens to hundreds of meters. Major minerals in the pegmatites are quartz, K-feldspar, albite, muscovite, garnet, tourmaline, beryl, Li-phosphate, and apatite (Alfonso and Melgarejo 2008). From a hydrogeological perspective, these rocks are of low hydraulic permeability with a porosity related to schistosity and the multiple sets of fractures associated with these high deformation areas. Furthermore, the lithological heterogeneity of this unit and its complex structure determine areas of distinct hydrogeological behaviour that may result in some confinement at depth. Due to the difficulty of tracing its internal structure, it is hydraulically considered as a continuous, rather homogeneous unit, at regional scale. Its recharge is mainly attributed to rainfall with no lateral flows from nearby units.

– *Hydrogeological unit in igneous rocks*. The Paleozoic sedimentary sequence was intruded during the Carboniferous-Permian periods by a large mass of granodiorite with quartz, plagioclase (oligoclase), K-feldspar with biotite and hornblende, that are cross-cut by dikes with associated sulfide mineralization. Oligoclase constitutes 42% of the granodiorite and has a Na/Ca molar proportion between 9/1 and 7/3 (ITGE 1994b). It forms the southern slope of the Rodes range and is overlain by the metasedimentary sequence by La Valleta thrust fault. Several bands of schists, linked to the intrusion process, appear within the granodiorites. Being low permeabil-

ity rocks, porosity is given by the fracture network that produces some flow priority directions as indicated by several permanent springs at Pau (PAU06) and Palau-Saverdera (PSV01). Similarly, rainfall is the main origin of its recharge.

– *Hydrogeological units in recent sedimentary formations*. Minor units constituted by alluvial and colluvial deposits originated at the Albera and Rodes ranges and cover the hanging wall block of the Garriguella-Roses fault. Their maximum thickness is estimated to be 10–12 m. They are unconfined aquifers with medium-high hydraulic conductivity that recharge mainly from rainfall and stream flow, yet they may receive some upward recharge from its basement. Laterally, these sedimentary formations connect to the present wetland areas of the Aiguamolls de l'Empordà Natural Park near the Mediterranean coastline. Alluvial and colluvial deposits are of low hydrogeological relevance at the regional scale and they may become dry during the summer months. They neither interfere with nor contribute to the hydrogeological system linked to the Vilajuïga water.

Tectonic structures are relevant to the groundwater flow in the entire system. On one hand, the normal Garriguella-Roses fault stands as the limit between the Pyrennes and the Empordà basin, and its hydrogeological relevance lies in the fact that both blocks have metamorphic and igneous rocks, so the whole regional flux takes place in these two hydrogeological units. On the other hand, La Valleta fault continues along the plain as indicated by the outcrops of metamorphic and igneous rocks among the Quaternary sedimentary formations (Figs. 2 and 3). More importantly, the thrust plane of La Valleta fault, with an estimated dip of 5–7°, developed over a layer of ampelitic shale which is assumed to be continuous along the thrust line, as it can be observed in the vicinity of Vilajuïga and in well logs.

The few available wells, especially in the mountainous area, do not permit drawing a potentiometric map. As a general report, most of the productive wells in the basin area are drilled to a depth between 40 and 120 m, the most productive levels being between 40 and 80 m in depth. Potentiometric levels usually rise up to 2–5 m below the terrain surface according to their owners; moreover, a presently closed well was reported to be flowing for a few months after drilling with high mineralized water. Boreholes in the igneous rocks located in the basin area are mostly unproductive, pointing out the occurrence of unweathered rock blocks among the fracture network in this hydrogeological unit. Furthermore, two wells near the Garriguella-Roses fault in the western part of the study area (sampling points GAR05, GAR06; Fig. SM2 in the ESM and Fig. 2) exploit water with a high hydrogen sulfide gas content similar to the natural H_2S-rich spring of Sant Climent Sescebes (SCS32). Well GAR05 has
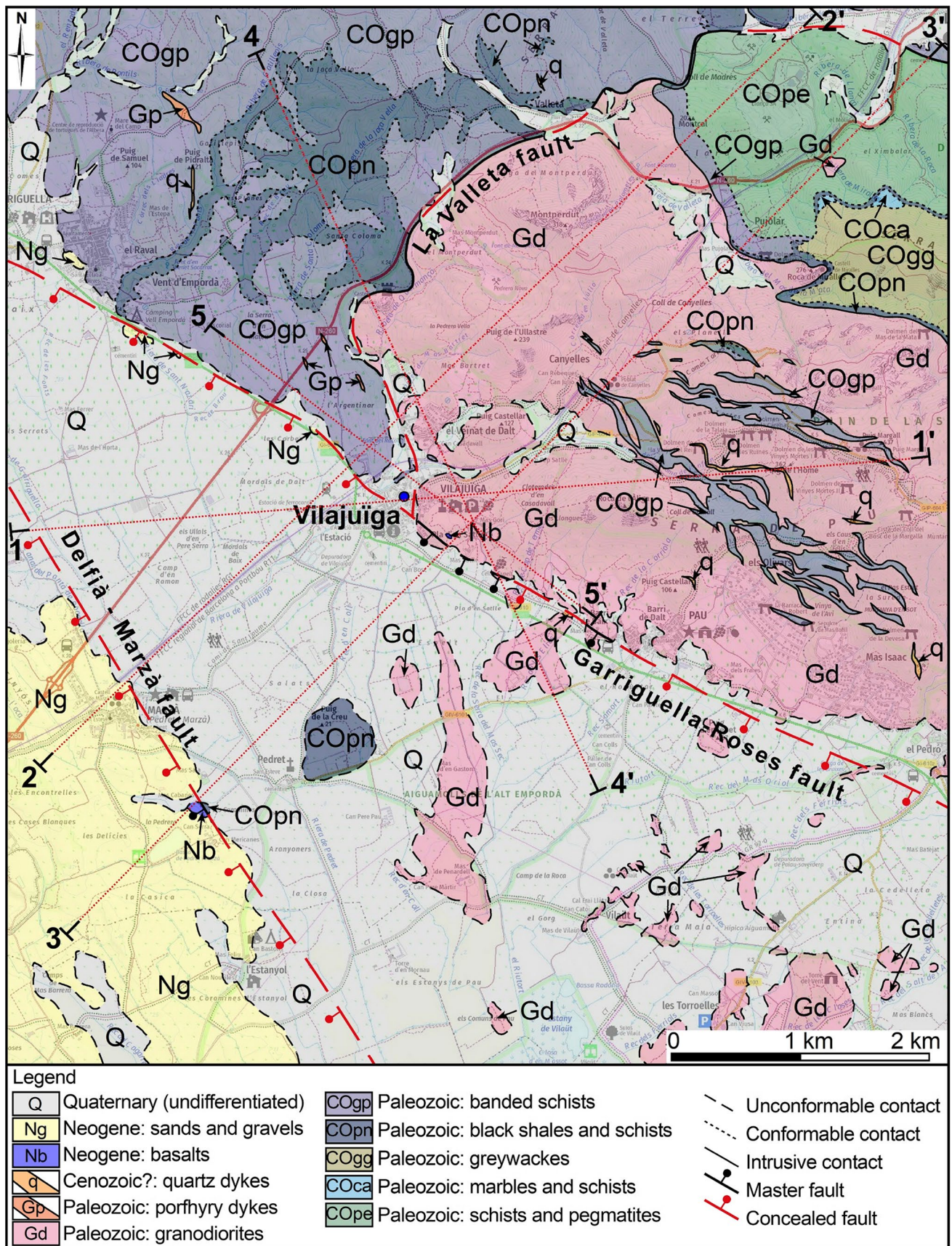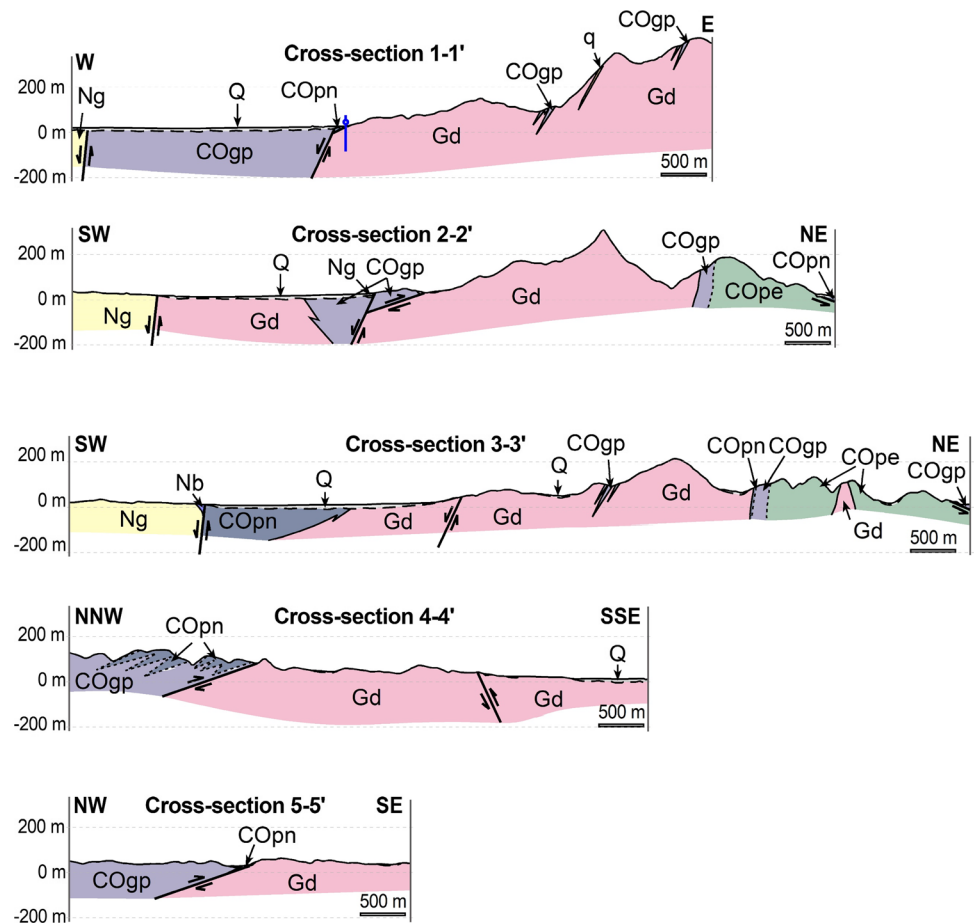
Fig. 2 Geological map of the study area, modified after ICGC ([2022](#))

Fig. 3 Geological cross-sections of the study area. Locations and legend are indicated in Fig. 2

been continuously flowing since its drilling in 2005. Finally, the potentiometric level at well Grifols (VIL01) was reported at 10 m below the surface after the borehole drilling—i.e., at 22 m above sea level (asl).

This short summary of the hydrogeological features of the area indicates the confined character of the productive zones, the occurrence of productive layers at a distinct depth as a result of the complex geological structure of the metamorphic and igneous rock units, and the relevance of fractures in the flow system, specifically in igneous rocks. Regarding the role of the Garriguella-Roses fault, (1) wells near it in the NW part of the study area produce H_2S-rich waters, (2) at the intersection of the Garriguella-Roses and La Valleta faults in Vilajuïga, CO_2-rich waters occur, and (3) moving in the SE direction, just a few hundred of meters away from Vilajuïga, wells and springs located in the igneous rock unit close to the fault show no traces of either hydrogen sulfide or carbonic acid in their composition.

Local geological features using ERT

Four ERT profiles provide a local view of the geology around the Vilajuïga exploitation wells, especially regarding

the location and structure of the main faults associated with its occurrence (Fig. SM1 in the ESM and Fig. 4). ERT-01 was conducted between the two exploitation wells, Escaire and Grifols, and it shows an upper layer formed by colluvial deposits (silty sand and gravel; 15–150 Ωm) down to 5–6 m depth overlying a 7-m-thick layer of a dark sandy clay and ampelitic black shale with a high water content (25–60 Ωm), as described by nearby well logs and directly observed in a trench. In the same trench, this shale overlays a drier, compact shale unit with a mylonite-like texture. In well Grifols, the ampelitic shales show a maximum apparent thickness of nearly 30 m overlying igneous rocks (granodiorite). A detailed observation of a hand sample of the ampelitic shale shows fragments of highly crushed black schist with fragments as much as 8 mm in size, and secondary gypsum precipitation as a result of pyrite oxidation, which has been observed to be unweathered in the trench. This shale is included in the Cambro-Ordovician stratigraphic series of the Albera range.

The complementary ERT-02, conducted in an E–W direction just north of well Grifols, identifies the geological contact between the igneous (granite in the eastern part; 40–300 Ωm) and the metamorphic (schists and slates in the western

Fig. 4 Electrical resistivity tomography (ERT) profiles performed in the vicinity of Vilajuïga village and close to the Vilajuïga water exploitation wells. Locations are plotted in SM1 in the ESM
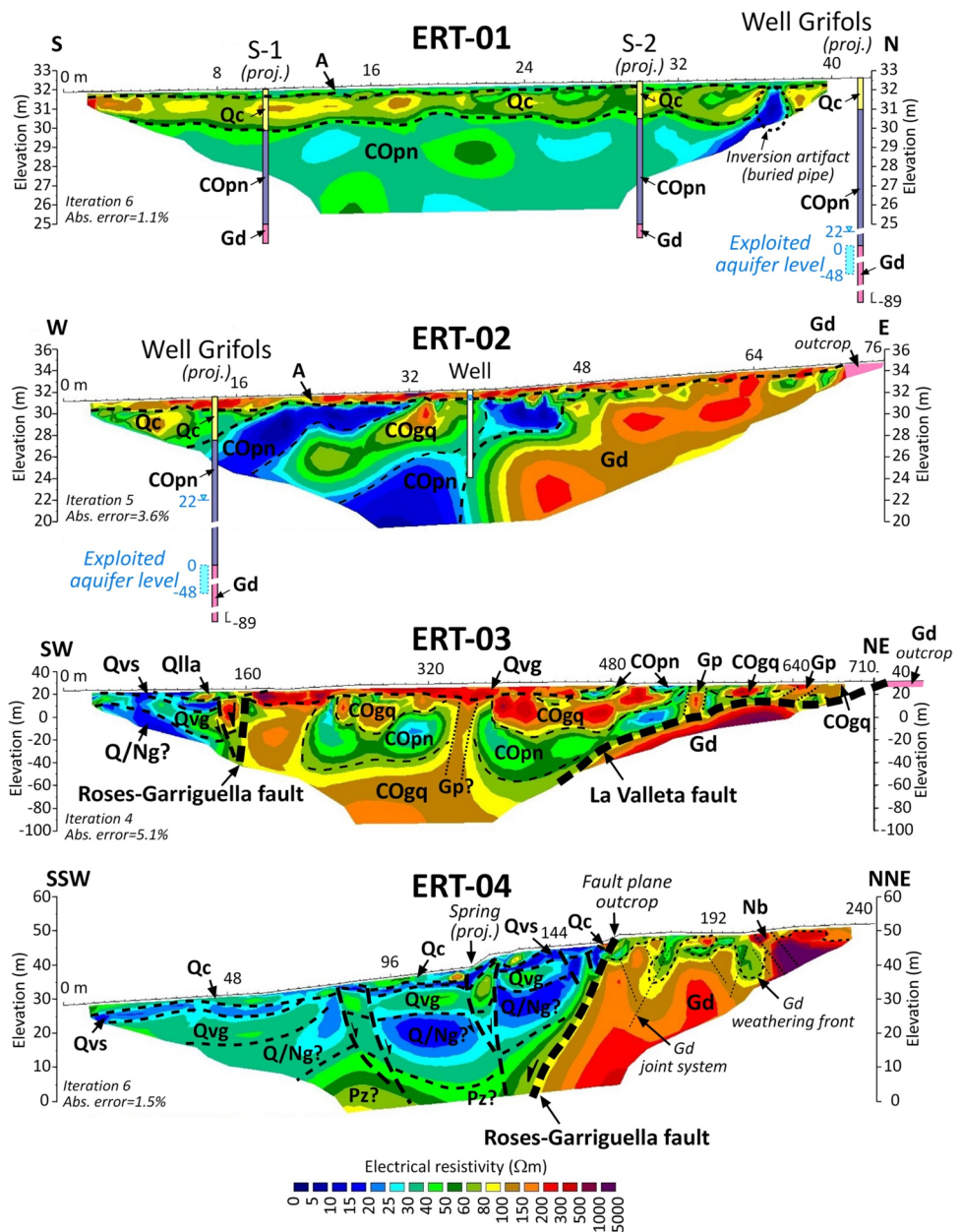
part; 4–30 Ωm) rocks. Granites are fractured and weathered, and the shales present an inner discontinuity with larger resistivity (100–200 Ωm). These data are supported by log observations from a nearby private shallow well, the water of which is slightly sparkling according to its owner, yet the well gets dry in summer, due to the recharge seasonality and the effect of declining water levels caused by the Vilajuïga water exploitation wells. The geological contact, attributed to La Valleta fault, has a strong vertical component in this shallow ERT profile, which is understood as a local detail. ERT-03 identifies the trace of La Valleta fault as a subhorizontal geological contact between two lithologies of distinct resistivity: schists and shales on the top (25–60 Ωm) and granite at the bottom (200–1,200 Ωm). This regional thrust

plane is continuously identified at 90 m below the soil surface and with a dip between 20 and 40°.

Finally, ERT-04, SE of Vilajuïga, clearly identifies the trace of the Garriguella-Roses fault with igneous rocks: granite (80–500 Ωm) and its weathering at the surface (30–80 Ωm) on the footwall block on the NNE side. Layered colluvial deposits (<60 Ωm), undefined on a high-resistivity unit attributed to igneous or metamorphic rocks (80–100 Ωm), appear in the hanging wall block. The fault has a dip of 60–70° and shows a wide damage zone also identified in the ERT profile by a lower resistivity contact. On the footwall block, a basaltic dyke (>8,000 Ωm), unknown to date, was identified and recognized in the field. The observation that the Quaternary colluvial materials present the same inner

resistance discontinuities suggests a potential deformation and a recent minor activity of the Garriguella-Roses fault.

Hydrochemical and isotopic results

The scope of using hydrochemical and isotopic data is two-fold: firstly, to determine the recharge origin, based on the water–rock interaction processes (plus their interaction with CO_2) and on stable isotope information; secondly, to estimate the water transit time which, together with the quality of the groundwater, may provide some indication about the system's vulnerability to potential changes, whether from an intense exploitation by nearby wells or due to climate change. The Vilajuïga water sample (code: VIL01), which is within the main scope of this study, gets special attention in this analysis. Groundwater samples are plotted according to the hydrogeological unit to which they belong, with sample VIL01 highlighted for clarity.

Groundwater hydrochemistry

The EC value for VIL01 is 2,140 µS/cm, which is twice as much as the EC of all samples with values ranging from 207 to 1,084 µS/cm, except sample GAR02 with an EC of 1,967 µS/cm, which is closer to VIL01. Nevertheless, while VIL01 has the largest HCO_3^-, Na^+ and K^+ concentrations, GAR02 is richer in Cl^- and Ca^{2+} (Fig. 5; Table SM2 in the ESM). Nitrate content is especially low, usually below 25 mg/L (0.4 meq/L), except for two samples.

The hydrochemical facies are diverse (Fig. 6). A main group of samples (group I) are in the mixed anion area, with a major percentage of HCO_3^-, SO_4^{2-} and Cl^- as well as in the mixed area with a variable dominance of Ca^{2+}, Mg^{2+} and $Na^+ + K^+$. Group II has a major HCO_3^- content with a significant fraction of SO_4^{2-}, and a dominant Na^+ content. Sample VIL01, with a clear HCO_3^-–Na^+ facies, jointly with samples from the Albera range plus GAR01 and GAR05, is close to group II. Sample VIL01 facies, jointly with its high EC, neatly reflects the influence of the CO_2 contribution. All other samples located in the plain surrounding Vilajuïga belong to group I, independently of whether sampling wells are drilled in metamorphic or igneous rocks.

Finally, samples from the fluvio-deltaic aquifer plot near group I, except sample CST25 which has a Cl–Na facies, yet low sulfate and magnesium contents indicate that seawater contribution does not fully explain its geochemical features. Its closeness to the Delfià-Marzà fault, its depth (72 m), and the smell of hydrogen sulfide in the well (also observed in samples GAR05, GAR06 and SCS32) suggest that deep groundwater fluxes from the basement are recharging this sedimentary unit.

A high partial pressure of CO_2 governs the chemistry of Vilajuïga water. Considering the CO_2–H_2O–$CaCO_3$

system (Fig. 7), samples cover a wide range of pH values (6.44–8.75), with VIL01 being the one with the lowest pH (6.44) and the highest free CO_2 (440 mg/L) and, consequently, the highest CO_2 partial pressure ($P_{CO2} = 0.38$ atm; Tables SM2 and SM3 in the ESM). Figure 7 shows that most of the samples from wells drilled in igneous rocks are unsaturated with respect to calcite, which is consistent with the composition of rock-forming minerals, among them oligoclase. Consistently, they show low Ca^{2+} and HCO_3^- concentrations. Unsaturation and consistently large P_{CO2} (0.01 atm) values suggest local-scale fluxes originated in the nearby Rodes range. Conversely, samples from wells located in metamorphic terrains show calcite-saturated conditions and a wide range of HCO_3^- values. The occurrence of marble layers and veins of reprecipitated calcite are potential sources of calcium, and dissolved CO_2 evolution takes place according to closed system conditions. Samples from the Albera range, sampled in 2014 (Table SM1 in the ESM), plot jointly with those from metamorphic rocks in the study area, pointing out that they belong to regional flow paths that permit soil CO_2 removal, due to longer water–rock interaction. pH values larger than 8.0 also reflect acid consumption by silicate weathering. Equilibrium is rarely attained (Table SM3 in the ESM). VIL01 sample is clearly differentiated from the rest of the data as the only CO_2-rich water in the dataset. Its high P_{CO2}, above usual soil values, indicates its geogenic origin, yet the lack of noble gas isotope data does not allow determining its precise origin, whether mantle or crustal (e.g., Ascione et al. 2018; Gilfillan et al. 2019; Karolyté et al. 2019; Defourny et al. 2022). This high partial pressure results in low pH and, therefore, in a high weathering capacity under open system conditions.

The Piper plot in Fig. 6 shows that groundwater from metamorphic as well as igneous rocks has high Mg^{2+} and $Na^+ + K^+$ proportions that restrict Ca^{2+} below 50% of the cation content. Calcium origin in metamorphic rocks is attributed to the occurrence of marbles and calcite veins, while in the igneous rocks it is attributed to the oligoclase composition ($7/3 < Na/Ca < 9/1$; ITGE 1994b), although cationic exchange with clays may also offset the proportion between these two cations (Fig. 7). The Ca:Na ratio for VIL01 is similar to that of two groundwater samples from metamorphic terrains—GAR01 and GAR05, the latter a very deep (460 m) artesian flowing well—and CST25 from the fluvio-deltaic formation, previously highlighted because of its potential relation with large-scale regional flow systems. Magnesium origin is linked to the weathering of biotite and hornblende; moreover, VIL01 also has an unusual K^+ content (25 mg/L; Table SM2 in the ESM) attributed to the K-feldspar, biotite, and hornblende weathering in a highly acidic environment.

Fig. 5 Relationship between electrical conductivity and distinct major hydrochemical components and **a** Chloride, **b** Bicarbonate, **c** Sulphate, **d** Nitrate, **e** Calcium, and **f** Sodium
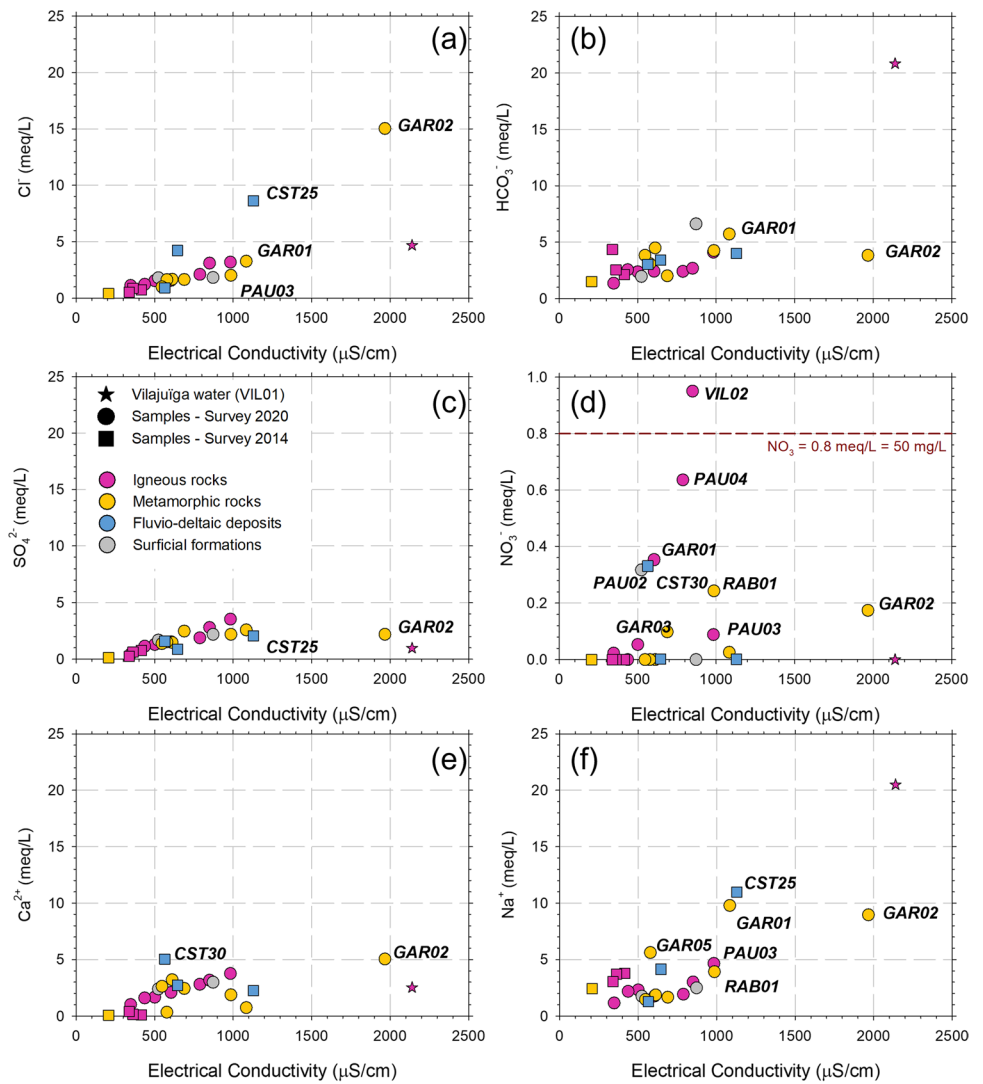
Trace elements

The most frequent trace elements of major geochemical relevance detected in groundwater are B^-, F^-, Li^+, Sr^{2+} and Ba^{2+} (Fig. 8; Tables SM4 and SM5 in the ESM), yet arsenic has also been detected in six samples with concentrations above 1 µg/L, but always below the World Health Organization threshold limit of 10 µg/L. Indeed, VIL01 has the highest values on B^-, Li^+, and Ba^{2+} as well as high concentrations of F^-, and Sr^{2+}. According to Hem (1985), fluoride, lithium and boron are common elements in pegmatitic rocks, which crop out in the area within the metamorphic rock hydrogeological unit. It is then relevant that sample VIL01 shows some of the highest concentrations of these elements.

Water isotope hydrogeology

Most of the samples from the study region are grouped in a small range of stable water isotopic values (Fig. 9), properly aligned with the Global Meteoric Water Line (GMWL), and VIL01 appears in the lighter limit of this range. The d-excess values show deviations from the GMWL, yet there is some uniformity around 10‰, consistent with local and present rainfall isotopic composition. Data from groundwater in igneous-rock wells show higher regularity (only PSV01 breaks this stability), while those from metamorphic rocks have larger variability. VIL01 shows a high d-excess value (11.24‰). Interestingly, data from the western part of the Albera range from the 2014 survey (DAR11, SCS32 and CAN02) show lighter isotopic ratios and larger d-excess values than samples from the Vilajuïga area, while those from the fluvio-deltaic aquifer are also lighter (except CST30) but with low d-excess values.

Altitudinal estimations of the samples' recharge areas are based on the altitude-isotopic line determined in the nearby Salines range, also located in the Eastern Pyrenees about 30 km westward from the study area (Brusi et al. 2011): Alt (m) = (−2663±191) − (481±30) $\delta^{18}O$, with

Fig. 6 Piper plot of the groundwater samples, differentiating those from the distinct hydrogeological units
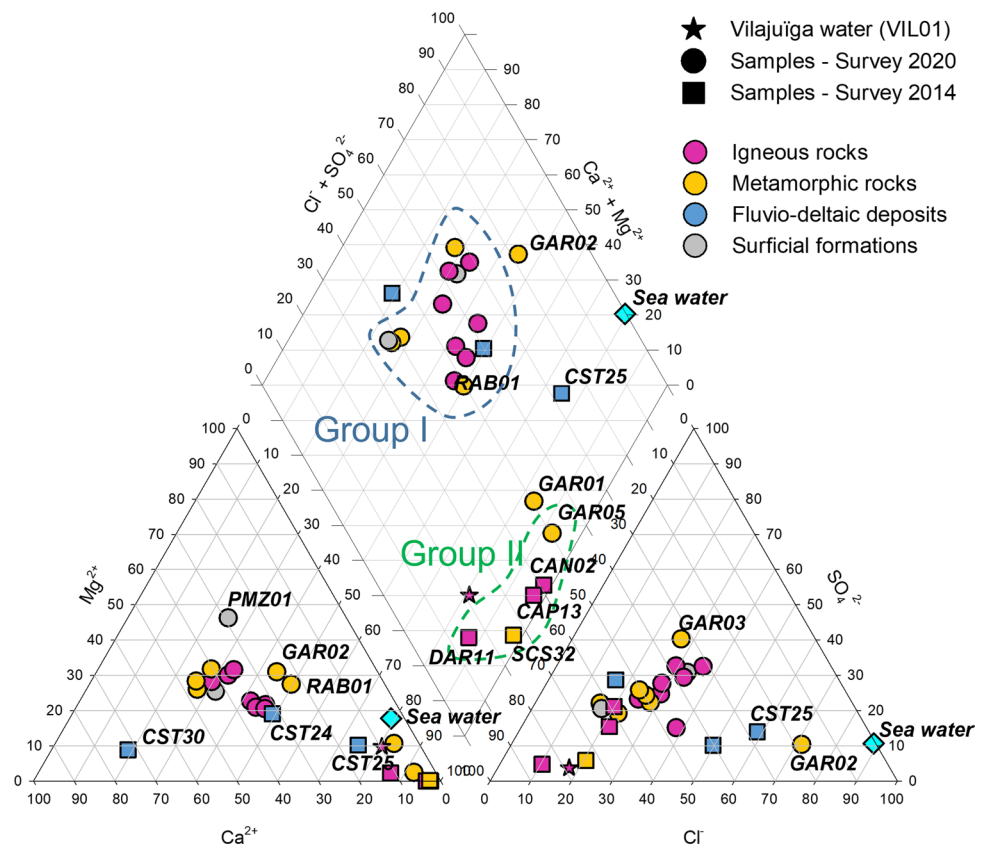

$r^2 = 0.952$. This indicates that most of the recharge takes place at altitudes between sea level and 400 m asl. Assuming the sampled wells in the study area have a depth of between 40 and 120 m, it can be assumed that they intercept large-scale regional flows that may originate at some even higher altitudes, consistent with the nearby orography which reaches up to 600 m asl. Conversely, samples SCS32 and CAN02 show recharge areas higher than 600 m asl, suggesting that their recharge may occur in the westernmost parts of the Albera range where higher altitudes are reached (Puig Neulós peak: 1,257 m asl). Samples obtained from the fluvio-deltaic aquifer are consistent with the recharge altitudes estimated for the study area around Vilajuïga: the Albera and Rodes ranges.

With regards to d-excess values, those above 12‰ are consistent with re-evaporated water and a certain continentality effect, which may correspond with the rainfall fronts originating in the Atlantic Ocean and that affect the Pyrenees, especially in its northern slopes. Conversely, samples without high d-excess values are related to local Mediterranean rainfall events, or a mixing of both with a larger local component. Low d-excess values shown by samples from the fluvio-deltaic aquifer layers could be associated with paleo-recharge under thermal and continental conditions distinct from the present ones (Gat 2010; IAEA 2013).

Tritium data from sampled groundwater were compared to the rainfall tritium content from 1961. The data were taken from the observatories of Avignon (France), Barcelona and Girona-Costa Brava Airport (which is located just 45 km south of the study area) to cover for the entire period 1961–2015 (GNIP database; IAEA/WMO 2021). Present annual tritium content from past precipitation was then estimated using a piston flow method (Fig. 10). Since details of the flow system are unknown, and therefore more exhaustive models (e.g., Małoszewski and Zuber 1982) are not possible, the piston flow approach is considered appropriate for the Vilajuïga hydrogeological system. Groundwater tritium content between 0.1 and 2.5 TU would be related to a recharge that occurred after 1980. Nevertheless, while samples with tritium values below ≈1 TU, among them VIL01, can be attributed to a recharge before 1960, no more precise information could be obtained for samples with higher tritium content as they can result from a variety of mixtures between pre-modern and modern waters. Obviously, the lower the tritium content, the "older" the recharge; yet a mixing between "modern" (after 1960) and "old" (before 1960) water can also be assumed. Finally, tritium was not detected in two samples from wells located in the metamorphic unit (GAR001, RAB01) and in the wells from the deepest accessible layers of the fluvio-deltaic aquifer (CST24 CST25, CST30).

Fig. 7 Plots of the CO_2–H_2O–$CaCO_3$ hydrochemical system. Although calcite is not a major mineral in the study area, these plots identify the effect of degassing CO_2 in the Vilajuïga water compared to other areas without the gas influence, and its effect on silicate dissolution (mainly plagioclase); **a** pH–Bicarbonate, **b** pH–Calcium, **c** log CO_2 Partial Pressure–Calcium, and **d** pH–log CO_2 Partial Pressure
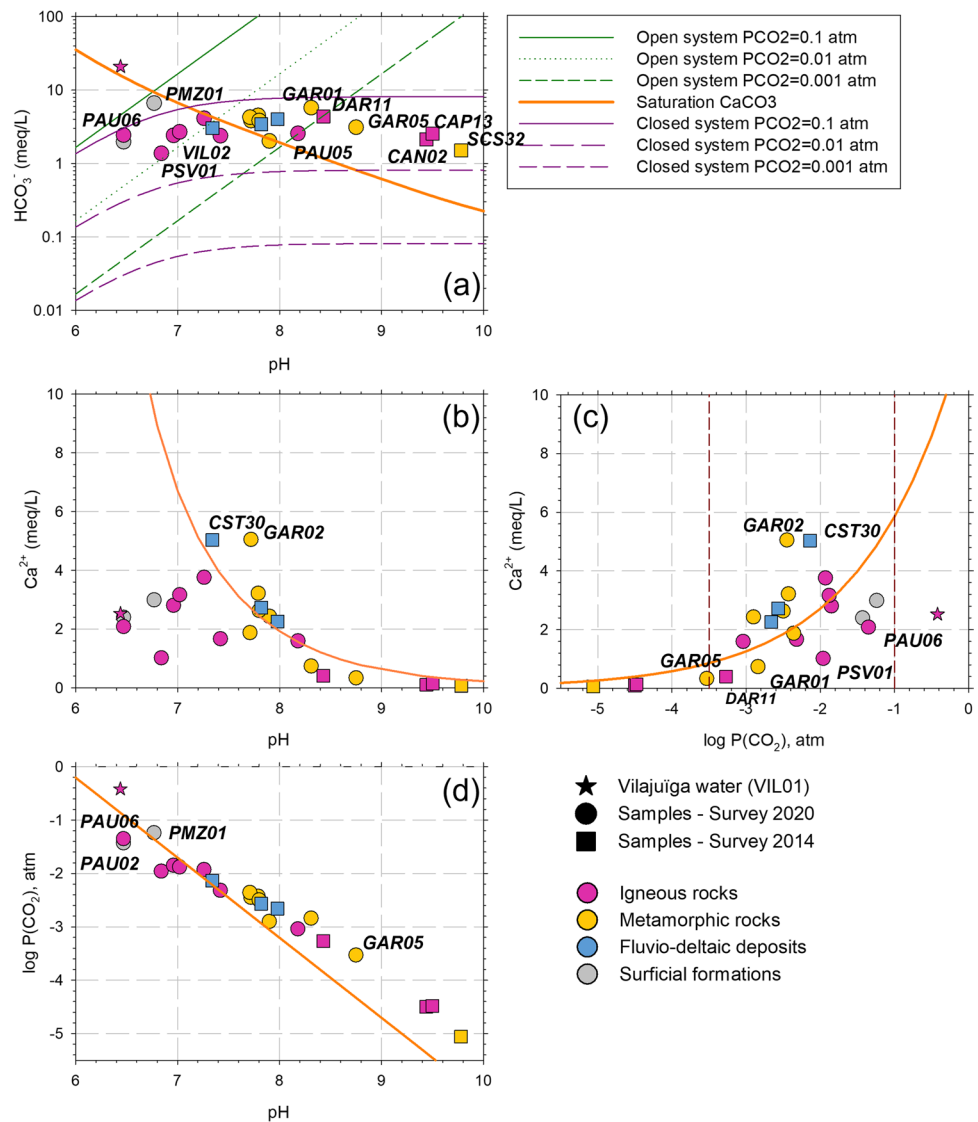
Carbon isotopes on DIC

Inorganic carbon stable isotopic data ($\delta^{13}C$) from eight samples, selected by their lower tritium content, offer a large range of results distributed along the usual groundwater range of −16 and −12‰ $\delta^{13}C$ values and increasing with their HCO_3^- content, with the VIL01 sample having the heaviest $\delta^{13}C$ and the highest alkalinity (Fig. 11; Table SM6 in the ESM). In this case, hosting rocks are mainly formed by silicate minerals, and these $\delta^{13}C$ values will later be discussed in terms of geochemical processes. Sample VIL01, the only one that portrays the influence of a high P_{CO2} in its composition, shows a $\delta^{13}C$ value of −3.3‰, pointing out a geogenic carbon contribution set at $\delta^{13}C$ values between −8 and −2‰ (Clark and Fritz 1997; Carreira et al. 2008).

Radiocarbon activity, $A^{14}C$, of these selected samples show low values (mean 19.5±6.2 pmC), and many of them lower than 10 pMC (Fig. 11; Table SM6 in the ESM),

indicating that the samples are mainly "old" groundwater. Uncorrected ages are in most cases meaningless, as processes affecting the initial radiocarbon activity ($A_o^{14}C$), such as fractionation, calcite dissolution or geogenic carbon addition, influence most of these samples. These considerations are addressed in detail in the 'Discussion' section.

Geothermometry

Attempts to estimate subsurface temperatures involve the use of several geothermometers—based on the assumption that waters are in equilibrium with certain minerals at the point of capture, that groundwater preserves its chemical characteristics during the ascent to the surface, and that minor or null mixing of groundwater from distinct origins occurs during sampling. Among the different existing geochemical relations for estimating temperature in origin, those based on

Fig. 8 Trace element concentrations in the groundwater samples: **a** Bromide, **b** Fluoride, **c** Lithium, **d** Barium, and **e** Strontium, expressed as their relationship with Chloride
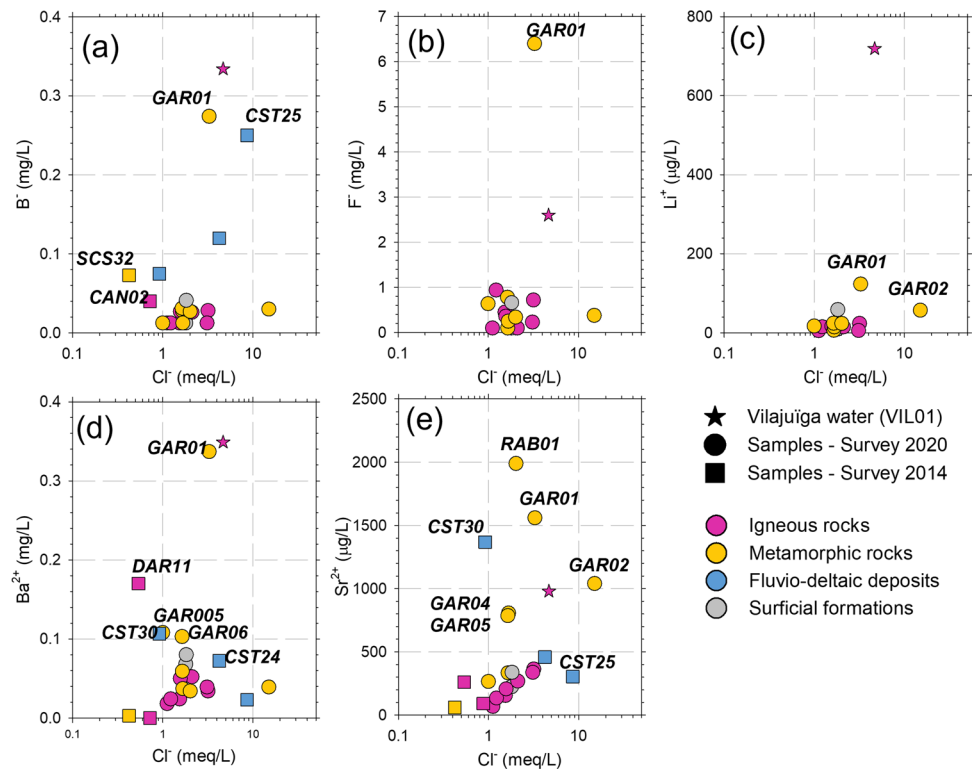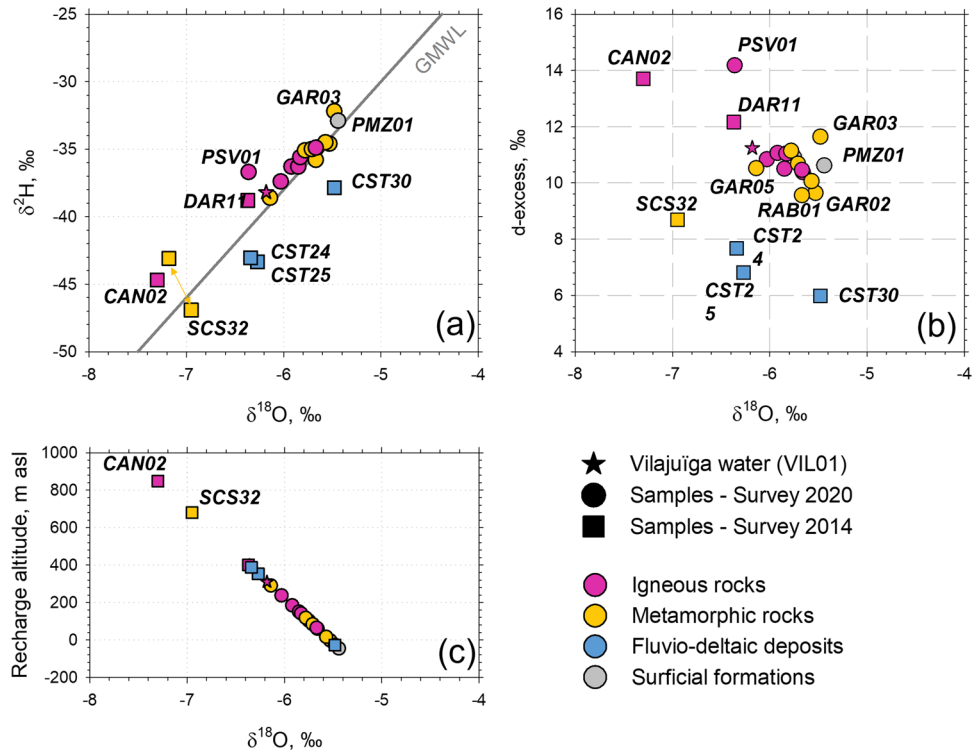

Fig. 9 Stable water isotopes data: **a** $\delta^{18}O$-δ^2H in reference to the global meteoric water line (GWML), **b** the d-excess value vs. $\delta^{18}O$, and **c** the estimated recharge altitude after the altitudinal isotopic line vs $\delta^{18}O$ as defined by Brusi et al. (2011)

the Na/K and K/Mg ratios (Giggenbach 1988) are the ones used in this study (Fig. SM3 and Table SM7 in the ESM).

Groundwater temperatures around 15 and 118 °C were estimated by the K/Mg geothermometer, with VIL01

showing a temperature of 14.7 °C (Table SM7 in the ESM). On the opposite end, calculated temperatures by the Na/K ratio were extremely high and variable, with temperature in samples from metamorphic rocks varying between

Fig. 10 **a** Tritium content in groundwater samples compared to the atmospheric tritium content since 1960 (GNIP database; IAEA/WMO 2021), and its actual concentration in 2020 according to a piston flow model. **b** Plot provides a large detail of the 2010–2020 period when sampling was conducted
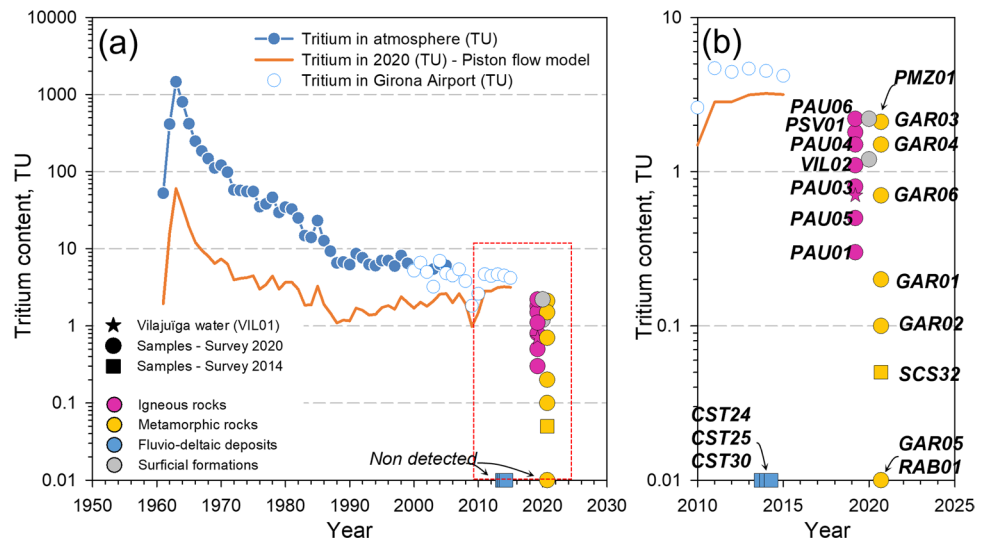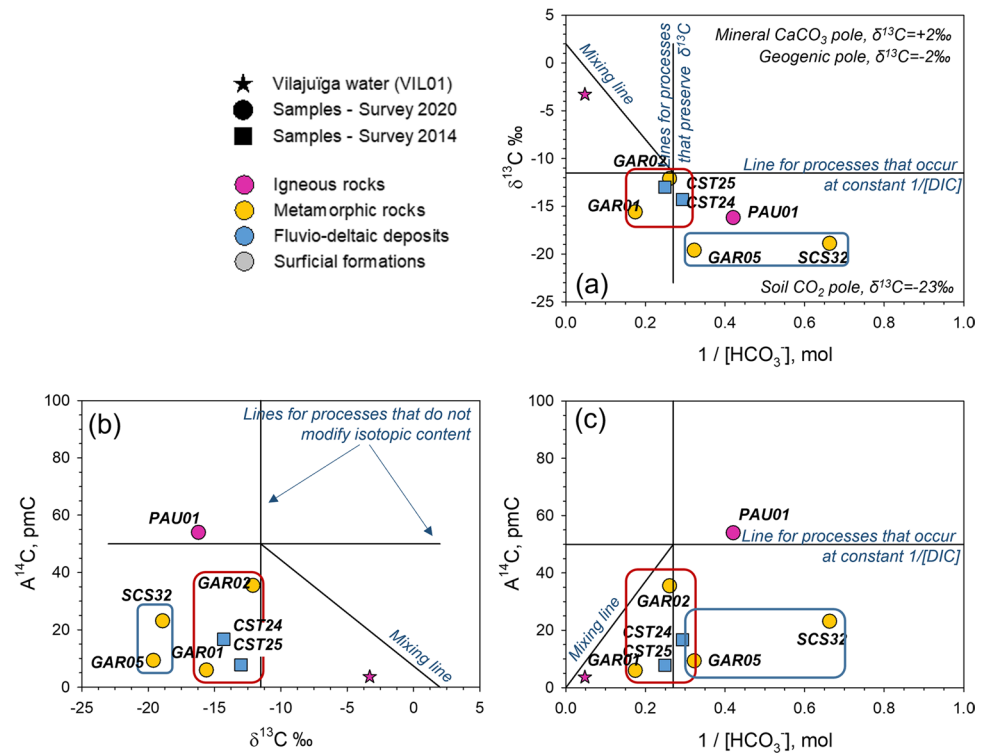

Fig. 11 Radiocarbon activity ($A^{14}C$), $\delta^{13}C$ values and HCO_3^- concentration using the plotting guidelines by Han et al. (2012) to evaluate predominant geochemical processes occurring in groundwater systems for radiocarbon dating: **a** 1/[HCO_3^-] vs $\delta^{13}C$, **b** $\delta^{13}C$ vs $A^{14}C$, and **c** 1/[HCO_3^-] vs $A^{14}C$

70–130 °C, reaching higher values of 160–220 °C for samples in igneous lithologies. Using both, VIL01 got temperatures of 14.6 and 187.6 °C, respectively. In the Giggenbach ternary plot (Fig. SM3 in the ESM), all samples lay within the field of immature waters, below the arbitrary line corresponding to a maturity index of 2.0, which indicates a low degree of rock–water equilibrium in the reservoir (Romano and Liotta 2020). Such discrepancies are likely to be attributed to uncertainties of geothermometers in natural water, where equilibrium has not been attained and additional processes such as mixing or, for instance, cation exchange, do

not meet the assumptions of the approach. Moreover, the lack of water-stable-isotope data right of the GMWL ($\delta^{18}O$ enrichment) suggests that water–rock interaction has not occurred, neither in the context of a geothermal system nor at high temperatures (Fig. 9; Gat 2010). Low pmC values and detectable tritium also support the idea of the mixing of distinct waters within this system.

Since no thermal activity has been identified in the area, the lowest range of values given by the K/Mg ratio with a mean temperature of 56.7±5.8 °C was taken as the most appropriate. Using a geothermal gradient of 32 °C/km

(ICGC 2022), an increment between a mean atmospheric temperature of 15 °C and an estimate of 50 °C, the likely depth attained by the groundwater flux, was less than 1 km below the surface.

Discussion

Recharge zone and groundwater flow paths

According to the orography and geology of the area, a recharge zone that contributes to the Vilajuïga spring is limited to the Albera and Rodes ranges, and its altitude is defined by the stable water isotope content below 600 m asl. The recharge zone mapped in Fig. 12 covers an area of 45 km² and it is consistent with the regional geomorphology providing a plausible interpretation of the flowing well GAR05 and other high-potentiometric-level boreholes drilled in the study area. This implies that infiltration reaches deep parts of the hydrogeological system that behave as confined aquifers. Its limits are defined by the complex structure

of the metamorphic rocks, as well as the distinct sets of fractures in both the metamorphic and igneous formations. The maximum depth attained by such flow lines is difficult to determine due to the geothermometry returning uncertain results, but it is hypothesized that it could likely reach a few hundred meters. The estimated depth of 1 km based on temperature data is considered as the highest potential depth given the regional geological framework.

Such proposed groundwater flow paths must consider the role of the two main fractures of the zone and explain their influence in the overall flow field, as well as on the singular occurrence of the Vilajuïga water in particular. The geological sequence of the present tectonic setting is described in Fig. 13, which points out that the crossing of both structural elements creates an intense fractured spot that ends up creating a zone of larger hydraulic conductivity. Indeed, the damage zone along the Garriguella-Roses fault plane has a vertical displacement of several hundred meters. Therefore, the igneous rocks in the footwall block (on the Pyrenees side) will be in contact with the metamorphic rocks of the hanging wall block (on Empordà basin side), along

Fig. 12 Main flow lines from the Albera and Rodes ranges and estimated recharge area for the Vilajuïga water (VIL01). General geological information can be obtained from Fig. 1

Legend

— Water divide

- - - Regional fault

→ Groundwater flow line

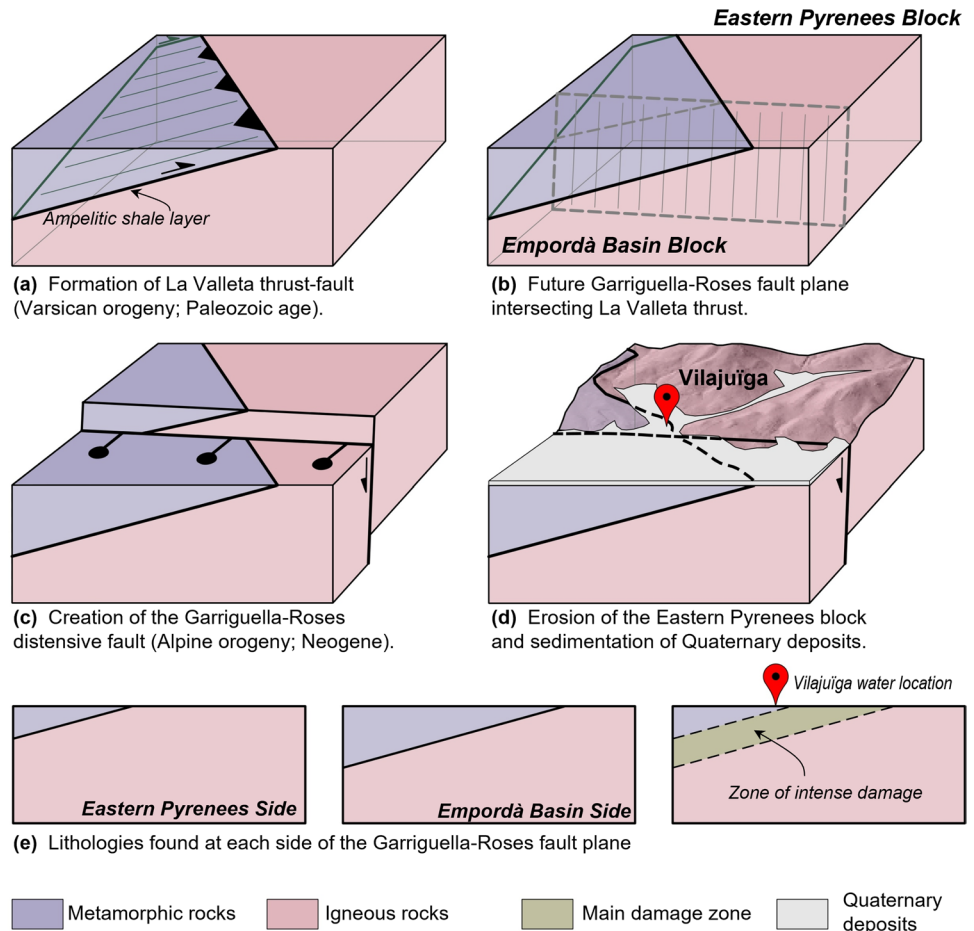◯ Proposed recharge zone for the Vilajuïga water
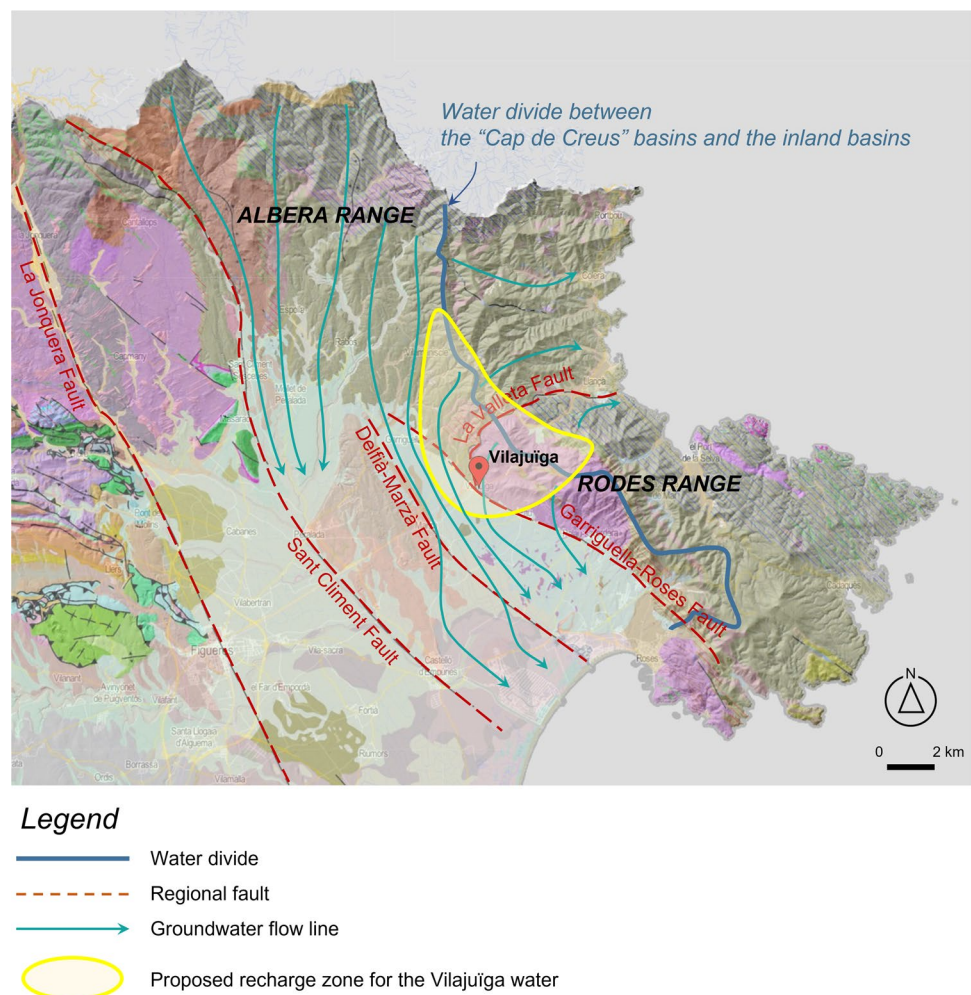
a wide strip as depicted by Fig. 13e. The contrast between the mechanical properties of both lithologies enhances the intensity of the fractures along the plane, with hydrogeological consequences. In particular, it connects the surface with confined aquifer zones existing at depth, as revealed by field observations of flowing artesian wells and high potentiometric levels. With regards to La Valleta thrust, the role of the ampelitic shale layer that acts as the plastic décollement material is relevant, as it defines a lithological ramp of low permeability that controls the regional flow field as described later in this section.

Considering the Garriguella-Roses fault, the high hydraulic permeability zone that develops along its fault plane, permits the discharge of H_2S-rich waters in its NW reach, and CO_2-rich waters in Vilajuïga. The main processes of hydrogen sulfide formation are assumed to be bacterial sulfate reduction. Bacterial sulfate reduction utilizes SO_4^{2-} present in waters from pyrite oxidation. Sulfate reduction takes place in the presence of organic matter, producing HCO_3^- and H_2S. The process of bacterial sulfate reduction occurs at a lower temperature range: 60–80 °C. In general, this process does not apply to those gases where the hydrogen sulfide content exceeds 5% (Appelo and Postma 2005; Matyasik et al. 2018). Indeed, metamorphic rocks, with the reported occurrence of sulfides (pyrite, chalcopyrite, arsenopyrite, etc.; ITGE 1994a, b) and the ampelitic shales that contribute along with organic matter are appropriate hosts for H_2S-rich springs (SCS32) or wells (GAR05, GAR06). Conversely, CO_2-rich water only outcrops at Vilajuïga, indicating a deep gas source that feeds groundwater at a single point or in a small area around Vilajuïga. It is hypothesized that the intersection of the two main faults (La Valleta and Garriguella-Roses) provides the necessary damage intensity in the fault plane to let the gas flow reach near-surface levels (Barros et al. 2021). This crossing also separates the NW part of this fault with the necessary conditions for H_2S-rich groundwater from the SE reach, mainly composed of igneous terrains, where feldspar dissolution will dominate and no evidence of CO_2-enriched geochemistry is found. At the crossing of both structures, CO_2 emanations highly alters the original groundwater composition.

The geochemistry of the Vilajuïga water (VIL01) is a mix of hydrogeological facies consistent with the weathering of metamorphic rocks (Fig. 6), with features corresponding to igneous rocks and pegmatitic bodies (Figs. 6 and 8).

Fig. 13 Block diagrams of the evolution since the Variscan orogeny of the structural setting of the Vilajuïga area in four steps (**a**–**d**). Diagram (**e**) represents the different lithologies on each side of the Garriguella-Roses fault that, because of their distinct mechanical behaviour, create a particular zone of intense damage along the fault plane that facilitates CO_2 degassing and the emergence of the Vilajuïga water

(a) Formation of La Valleta thrust-fault (Varsican orogeny; Paleozoic age).

(b) Future Garriguella-Roses fault plane intersecting La Valleta thrust.

(c) Creation of the Garriguella-Roses distensive fault (Alpine orogeny; Neogene).

(d) Erosion of the Eastern Pyrenees block and sedimentation of Quaternary deposits.

(e) Lithologies found at each side of the Garriguella-Roses fault plane

Nevertheless, high P_{CO2} increases the alteration rates and, therefore, modifies VIL01 hydrochemical characteristics in comparison with nearby samples. A proposed conceptual model for the Vilajuïga water flow field is portrayed in Fig. 14, which distinguishes two groundwater contributions with the first being that of the metamorphic rocks, recharged at the Albera range (blue arrows in Fig. 12), which move upwards according to the ramp formed by the ampelitic shales. This layer has an apparent thickness of up to 30 m, as reported by well logs, and is of very low hydraulic conductivity, as observed in the outcrops of a large-diameter excavation (Espai Misteri; Fig. SM1 in the ESM) in the vicinity of the Vilajuïga water producing wells. A second contribution originated in the Rodes range, consisting of igneous rocks (orange arrows in Fig. 12) which move towards the Garriguella-Roses fault and flow below La Valleta thrust. At depth, both flows mix and are affected by CO_2, modifying its geochemical features at the specific location where gas moves towards the surface. This conceptual model considers that the damage zone creates an area of higher hydraulic conductivity that allows for deep groundwater flow, probably in confined aquifers, and reaches the surface, similar to a piezometer. The Garriguella-Roses fault is not seen as a barrier that forces an upward groundwater flow from the mountain range, impeding its continuity to the basin block. Indeed, the coexistence of two lithologies on each side of the fault in its upper part (Fig. 13) increases the connectivity, and the occurrence of igneous rocks on both sides of its lower part does not impede groundwater flowing through it.

Main cultivations (2,805 ha of total crop area; IDESCAT 2021) are cereals and forage (49.8%), vineyards (33.0%), olive groves (15.9%) and others (1.3%), which means that
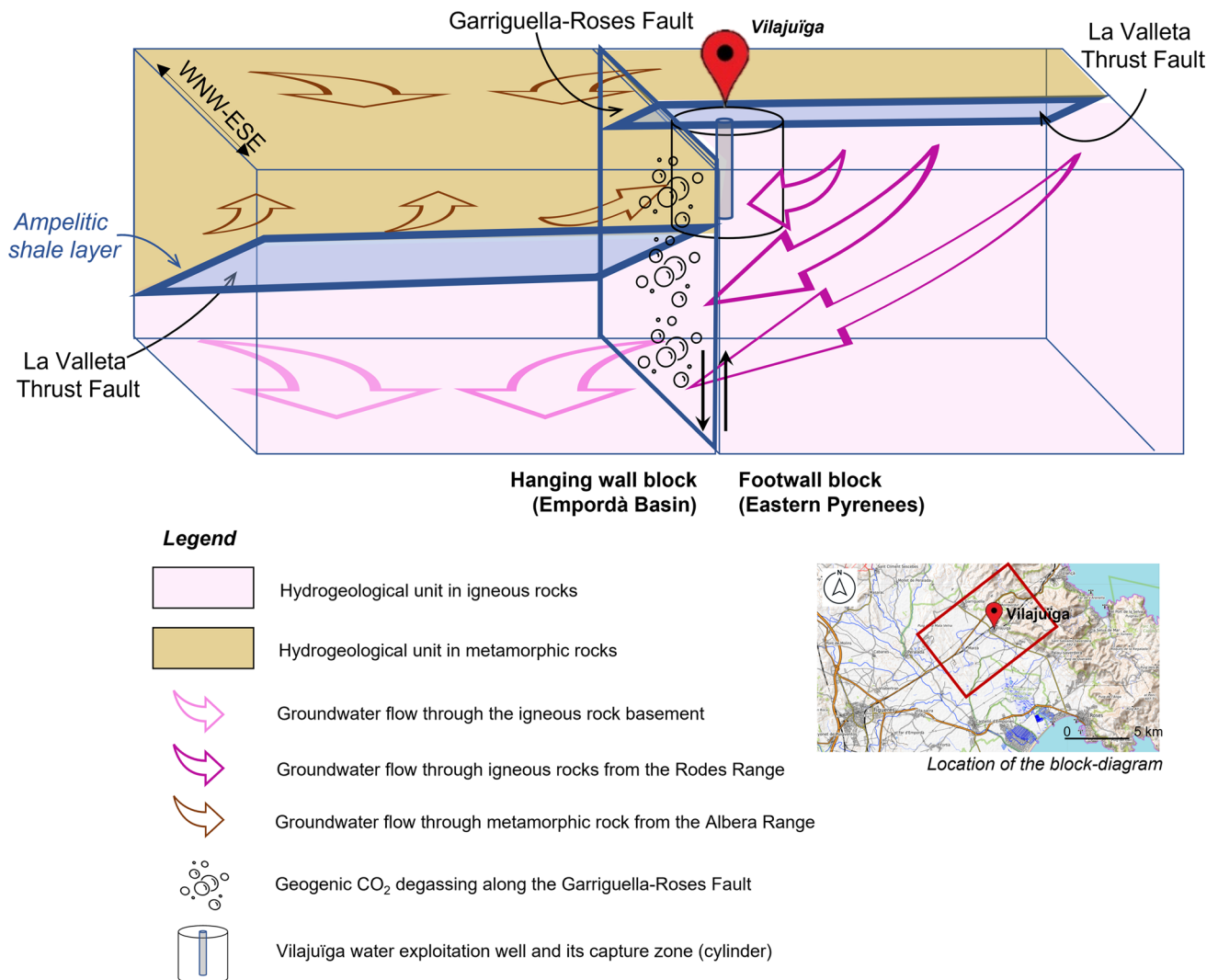

Fig. 14 Hydrogeological conceptual model of groundwater mixing in the vicinity of Vilajuïga considering the intersection of the two major tectonic elements: La Valleta and Garriguella-Roses faults. The distinct flow paths within the metamorphic and igneous rock aquifers are shown.

intensive fertilizer use (manure) only applies to half of the cultivated area. This is the reason why nitrate content is especially low, usually below 25 mg/L (0.4 meq/L), except for two samples. It also suggests that groundwater flow from recharge areas, located in the Albera and Rodes ranges with no agricultural land, is dominant in most wells, and in particular, it does not present a hazard for the Vilajuïga water quality. Nevertheless, low Eh values (Table SM2 in the ESM) in some wells is associated with nil nitrate values, indicating that potential denitrification environments may delete any trace of nitrogen inputs from the land surface.

Governing geochemical processes

At first glance, the sodium-bicarbonate hydrochemical facies of Vilajuïga water (Fig. 6) indicates the dominant role of the high P_{CO2} with its high alkalinity. With regards to sodium, oligoclase dissolution in igneous rocks would offer such high Na^+ content. However, stability diagrams point out that soil samples from metamorphic and igneous rocks lie on the boundary between Na-montmorillonite and kaolinite, suggesting that sodium richness is somehow characteristic of both of them and that their dissolved SiO_2 content is similar, as a result of silicate weathering (Fig. 15). Therefore, mineral-forming metamorphic rocks also produce Na^+ ions during weathering under closed system conditions (Railsback 1993), indicating that recharge takes place in both terrains, as postulated by the flow conceptual model. Furthermore, magnesium richness of about 30% of the cation molar mass (Fig. 6) is attributed to the dissolution of biotite and hornblende in igneous rocks, as well as of biotite, hornblende, muscovite and chlorite in metamorphic rocks, supporting the fact that groundwater samples from either hydrogeological unit have a similar hydrochemical facies.

Finally, local CO_2 geogenic contribution in Vilajuïga alters the whole hydrochemical composition of the mixing between groundwater from both recharge areas. It produces a re-equilibrium of the existing dissolved species, plus a higher weathering action due to a low pH in expected open system conditions (VIL01 pH = 6.44; Fig. 7). This higher capacity will mainly affect Na-feldspar (oligoclase), as pointed out by the large Na^+ content in solution.

The most frequently identified trace elements are B^-, F^-, Li^+, Sr^{2+} and Ba^{2+}, represented in Fig. 8 in relation to chloride as a conservative ion. The VIL01 sample has the highest values of boron, lithium and barium ions, as well as high values of fluoride and strontium in relation to the whole set of samples. Fluoride, lithium and boron are abundant in pegmatitic rocks (Hem 1985). In pegmatites, minerals such as hornblende, micas and apatite may have F^--replacing hydroxyl groups. Boron is associated with tourmaline and biotite, and minerals that contain lithium are also common in pegmatites, although at trace concentrations, and it usually
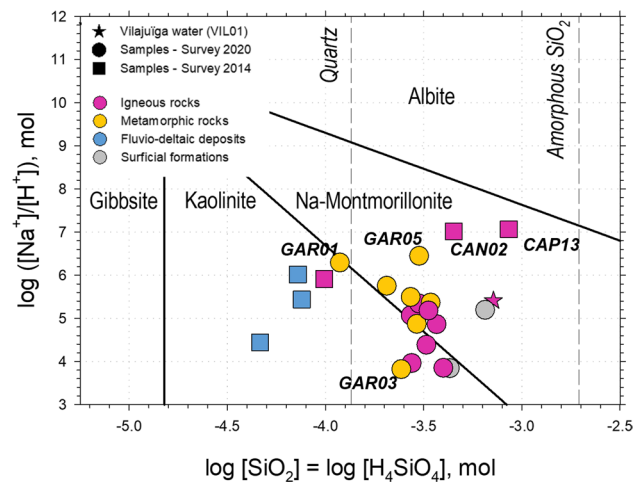

Fig. 15 Na-stability diagram of silicate weathering

remains in dissolution after the alteration of the mineral. It is therefore illustrative that the abundant elements in the VIL01 sample are associated with pegmatites and that, except in the case of GAR01, they do not appear with high concentrations at any other sampling point in the study area. Pegmatites present relevant intruded bodies in the metamorphic rocks cropping out on the northern slope of the Rodes range (Fig. 2), yet their distribution in depth is unknown. Nevertheless, the abundance of lithium and boron permits tracing the groundwater flow exploited by well VIL01 back to these pegmatitic masses, extending the recharge zone beyond the hydrographic divide (Fig. 12) and, because of their occurrence in well GAR01 as well, supporting that the Garriguella-Roses fault does not act as a barrier for groundwater fluxes towards the Empordà basin.

The presence of another trace element, Ba^{2+} is generally controlled by the dissolution of barite ($BaSO_4$), which is usually found in medium- and low-temperature hydrothermal dykes with accompanying metal sulfides, as is found in the Les Gavarres range (Roqué and Pallí 1994). Barium also appears in small amounts in the feldspar structure replacing potassium, calcium or sodium. Again, VIL01 and GAR01 show similar Ba^{2+} concentrations, as much as four times the usual value, pointing out that despite being located in distinct hydrogeological units, the Garriguella-Roses fault permits groundwater flow through it. Strontium usually replaces calcium or potassium in minerals of felsic igneous rocks (e.g., granodiorites); although, in the study samples, the highest concentrations of strontium, including that of VIL01, are associated with samples of wells drilled in metamorphic rocks. This is attributable to the cation exchange capacity of smectites, such as montmorillonite (a product of silicate minerals weathering), with strontium ions available (Deer et al. 2013). With regards to strontium, VIL01 relates more to samples in the metamorphic rock unit than to those

in the igneous rock unit, sustaining the mixing described by the conceptual model for the Vilajuïga water.

Dating Vilajuïga groundwater

Tritium content indicates that samples with TU < 1, including VIL01, represent a mixing of groundwater recharged during the prebomb era (i.e., before 1960) with some contributions from most recent recharge inputs. Otherwise, samples with TU > 1 were recharged any time after 1960 or they are a mixture of flow lines with distinct transit times (Fig. 10). This interpretation is consistent with the proposed conceptual model. Moreover, the fact that some samples are tritium free (0.0 TU), especially those located at the fluvio-deltaic formation, representing the regional discharge of the hydrogeological system, indicates the large magnitude of the overall hydrogeological system and that other dating methods, such as radiocarbon, are needed to estimate Vilajuïga groundwater age.

Within silicate hosting rocks, groundwater carbon sources in all samples, except VIL01, derive from soil CO_2, so the biogenic pole ($\delta^{13}C_{CO2}$ = approx. –23‰) dominates. Since no major contributions of calcite dissolution are expected, as reflected by the low Ca^{2+} content for most of the analysed samples (Fig. 7), the recharging dissolved inorganic carbon stable signature ($\delta^{13}C_{REC}$) will be close to that of the soil CO_2 under closed system silicate weathering conditions (Clark 2015). Nevertheless, some decrease of the $\delta^{13}C$ content is observed, which is attributed to different feasible processes: isotopic fractionation under early open system stages, dissolution of calcite re-precipitated in veins or from the marble units embedded in the metamorphic rock series, or to both processes concurrently. Accepting that calcite contribution will take place at depth, recharge $\delta^{13}C$ will be close to the initial $\delta^{13}C_{CO2}$. Therefore, the dilution estimation factor, q, was defined by Pearson (1965) and Pearson and Hanshaw (1970), as

$$q = \frac{\delta^{13}C_{sample} - \delta^{13}C_{cal}}{\delta^{13}C_{REC} - \delta^{13}C_{cal}} \tag{1}$$

and this can be applied using $\delta^{13}C_{REC} = -23‰$, $\delta^{13}C_{cal} = +2‰$. Isotopic C values and dilution factors are listed in Table 1. For the VIL01 sample, with a geogenic carbon contribution, $\delta^{13}C_{rock}$ is substituted by the $\delta^{13}C$ value resulting from the contributions of magmatic CO_2 and calcite dissolution. Assuming a geogenic gas contribution fraction of 0.65 ($\delta^{13}C_{geo}$ = –3‰) and a calcite fraction of 0.35, a $\delta^{13}C$ value of –1.25‰ will be used in place of the mineral pole, while recognizing that groundwater dates in cases with a high geogenic carbon contribution must be cautiously considered (Clark 2015).

Figure 11 is drawn following the guidelines given by Han et al. (2012) as a means to evaluate geochemical processes involved in groundwater radiocarbon dating. In detail, PAU1 represents a sample that preserves a $\delta^{13}C$ value close to the atmospheric CO_2, a low HCO_3^- content and relatively modern water ($A^{14}C$ = 54 pmC) consistent with water infiltrating in igneous rock terrains. All other samples can be grouped: (1) wells GAR005 and SCS32 (blue squares) are the result of a low contribution of mineral carbon (i.e., from calcite dissolution), and their low HCO_3^- content shows consistently low P_{CO2} values (Fig. 7) and large residence times; and (2) wells GAR01 and GAR02 from metamorphic terrains lie in the areas of the Han diagrams corresponding to the effect of weathering of silicates; therefore, there are no reactions with carbonates, nor radiocarbon decay. Finally, sample VIL01 lies near the line that represents a mixing between two inorganic carbon sources, namely soil CO_2 and geogenic CO_2, plus radioactive decay of the former.

Corrected radiocarbon ages distinguish two groups after the use of the dilution factor q (Table 1),

1. Groundwater samples with ages older than 10 ka years BP, especially GAR01 and GAR05, also including samples with no tritium content from the regional discharge area—CST24, CST25 and SCS32. The latter, with a very low tritium value, points out some minimum mixing with recent recharge. GAR05 belongs to the deepest well in the area (460 m) and it clearly represents a deep

Table 1 Tritium and carbon isotopic values for groundwater dating

Code	Tritium (TU)[a]	$A^{14}C$ (pMC)	Error (±) (pMC)	$\delta^{13}C$ (‰)	Factor q (%)	Corrected age (Years BP)
GAR01	0.2	5.94	0.06	–15.6	70.40	20,439
GAR02	0.1	35.50	0.13	–12.1	56.40	3,827
GAR05	0.0	9.30	0.1	–19.6	86.40	18,426
PAU01	0.3	53.97	0.2	–16.2	72.80	2,474
VIL01	0.7	3.61	0.05	–3.3	9.43	7,933
CST24	0.0	16.70	0.1	–14.3	65.20	11,260
CST25	0.0	7.80	0.1	–13.0	60.00	16,866
SCS32	0.05	23.10	0.1	–18.9	83.60	10,633

[a]Tritium values have a precision of ±0.1 TU, even for those values reported as 0.0 TU by the lab

part of the hydrogeological system. GAR01, on the other hand, is the oldest water sampled, only at 60 m depth, and takes advantage of the ramp created by La Valleta thrust which brings deep groundwater recharged in the Albera range along flow paths upward to the surface (Fig. 12).

2. Groundwater samples with ages younger than 10,000 years BP, among them VIL01. Samples GAR02 and PAU01 also indicate the same mixing from the recent recharge. GAR02, located in a similar geological setting as GAR01, captures more surficial, and therefore modern flow lines. PAU01, hosted in igneous rock, represents the recharge in the Rodes range with a shorter pathway and, consequently, a younger age. Vilajuïga water (VIL01) has an approximate age of 8,000 years BP. Because of its tritium content (0.7 TU), it is interpreted as a mixing between the deep flow lines intercepted by well GAR01 and the recharge from the Rodes range identified at well PAU01. Such mixing is consistent with the previous hydrogeological analysis and supports the idea that VIL01 is indeed a combination of recharge areas, whose hydrochemistry has been altered by the input of geogenic CO_2. The VIL01 radiocarbon age is a midvalue between older (GAR01) and younger (PAU01) recharges, which is consistent with the conceptual model. In this context, the dilution factor estimated for this sample looks reasonable despite the assumptions, yet the absolute age value must be taken with prudence.

Resilience and vulnerability of the Vilajuïga hydrogeological system

The singularity of a hydrogeological system, such as the Vilajuïga water, reflects a natural dynamic that may be affected by several human and environmental pressures or perturbations that modify the flow rate, the chemical composition of the resource, or its economic and heritage values. Up to now, periodic analysis of the Vilajuïga water hydrochemistry does not show any alteration of its original quality. Nevertheless, under the new scenario of water scarcity due to climate change in the Mediterranean regions (MedECC 2020), it is worth rethinking the effect of potential disturbances on this system. In this exercise, resilience is understood as the capacity of a system to respond to a pressure by resisting damage and recovering quickly; in other words, resilience refers to the chances that a system in a state of failure will return to a nonfailure state. Vulnerability is a term used to represent the natural ground characteristics that determine the ease with which a groundwater system may be altered by human activities, and it provides measures regarding the likelihood of failure due to such pressures (Rodak et al. 2013).

According to MedECC (2020), aquifer recharge will be strongly impacted by climate warming and reduced rainfall. Overexploitation of groundwater is likely to develop, having a greater impact on decreasing groundwater levels than climate change. Impacts on water resources of global warming levels higher than 1.5–2 °C by the end of the 21st century will be significantly stronger, substantially increasing the probability of more extreme and frequent droughts. An evaluation of climatic conditions in the Catalan coast foresees an increment of 1.4 °C of temperature and a rainfall decrease of 8.3% by 2050 (Calbó et al. 2016). Based on these predictions, Mas-Pla et al. (2016b) estimated the available water resources for each basin in Catalonia for Horizon 2050, based on a mass balance approach. For the Albera and Rodes ranges' watersheds, the ratio between available resources and predicted rainfall is presently 0.218, and it will be 0.173 by 2050. Considering that the present mean rainfall is 531 mm (2000–2015), foreseen rainfall will decrease to 487 mm, and resources will be at 73% of the present ones, with a loss of 31 L/m^2 of available resources, including both surface water and groundwater.

Based on this estimation, and assuming that recharge variation will be of the same order of the overall predicted water resources decrease, one is dealing with a hydrogeological system at a regional scale with a fractured porosity network and a long transit time (ca. 8,000 years). The time constant τ_c for an aquifer is defined as the time necessary for the effects of a change, such as a modification of the recharge, to achieve a permanent or balanced regime (Domenico and Schwartz 1998), and expressed by $\tau_c = S_s L^2/K$, where S_s is the storage coefficient, L the length of the domain, and K is the hydraulic conductivity. For the Vilajuïga water hydrogeological system with $K = 10^{-6}$ m/s, $S_s = 5 \times 10^{-4}$, and L between 6 and 8 km, the time constant value is 600–1,000 years, depending on the value of L. This means that a diminishing recharge will permanently influence potentiometric heads at the discharge area after several centuries. Therefore, no significant modifications of the regional flow field, and eventually to its water geochemistry, are envisaged because of environmental changes, compared to those derived from new climatic scenarios. In this sense, the system behaves as resilient and of low vulnerability in the face of these pressures. Nevertheless, an increase in groundwater withdrawal rates or pollution in nearby areas within the radius of influence of the production wells will threaten its vulnerability. To date, current exploitation rates do not present any threat to the quality of the Vilajuïga water since its hydrochemistry has remained uniform for the last 100 years. Further development within the delineated recharge area should prevent potential damage and restrict itself from affecting the economic, as well as the patrimonial values of this singular groundwater source. Despite the possible variance in vulnerability, it is postulated that the deep nature of the flow

field, the fact that it develops at a large scale under confined conditions, and the geogenic nature of CO_2 safeguard the dynamics of the system and keep its resilience within acceptable levels. The time constant value for a pressure occurring at a distance of 1 km from the production well is nearly 20 years, which means that a progressive decline of the potentiometric head due to intense pumping (assuming that the cone of depression is smaller than this distance) will take almost two decades to be noticed at the well; yet, if the impact occurs, it will take a similar time to recover after the pressure has been removed. Each pressure, of course, will need its own risk assessment, but the time factor provides an initial measure of the magnitude of the tragedy. Given the aforementioned economic and heritage value, continuous monitoring is necessary to track changes and anticipate impacts in spite of the system's tolerable resilience.

Conclusions

The hydrogeological conceptual model of the CO_2-rich natural water of Vilajuïga (NE Catalonia, Spain) relates the water's occurrence and unique quality to (1) a peculiar tectonic environment characterized by the intersection of two distinct structures, and (2) the upward flow of geogenic CO_2 at this specific location that determines the final geochemistry of the Vilajuïga water.

In synthesis, the origin of the Vilajuïga water reflects the sum of diverse geological factors. The La Valleta thrust fault, developed after a layer of ampelitic shales, allows an upward groundwater flow within the metamorphic rock hydrogeological unit with the recharge area located on the Albera range. Such discharge meets another groundwater flow generated at the igneous-rock aquifer formation of the Rodes range in the vicinity of the Garriguella-Roses fault, where both mix and interfere with the occurrence of geogenic CO_2. The conceptual model proposes that the distinct mechanical behaviour of the existing lithologies in each block of the Garriguella-Roses fault produces a major damage zone in the intersection with La Valleta fault that explains the limited spatial occurrence of the Vilajuïga water. The overall recharge area extends along the Albera and Rodes ranges at elevations below 600 m asl.

Despite both hydrogeological units having distinct lithologies, their hydrochemical facies do not differ as dominant silicate minerals are similar. Indeed, groundwater samples show a varied composition with different percentages of anions ($HCO_3 > SO_4 > Cl$) and cations ($Na > Ca \approx Mg$). Noticeably, the effect of degassing CO_2 only affects the Vilajuïga water, as no other groundwater samples show such a clear HCO_3–Na facies, which is an indicator of the extremely localized occurrence of CO_2 across the study area. Trace elements (B, F, Li), resulting

from the dissolution of pegmatitic rocks, differentiate Vilajuïga water from the rest of samples and it points towards its relationship with deep flow paths (<< 1 km) within the hydrogeological units. Nevertheless, the Garriguella-Roses fault does not act as a barrier that facilitates an upward groundwater flow. Conversely, its damage zone acts like a borehole (i.e., a narrow zone of high hydraulic conductivity) that permits the flowlines of deep groundwater to be captured by the exploitation wells.

Radiocarbon dating of Vilajuïga water requires some geochemical considerations due to the occurrence of geogenic carbon. After correction, a plausible age of 8,000 years BP is estimated. Tritium content in the Vilajuïga water sample indicates mixing between older water, as that in well GAR01, and younger contributions originated in the Rodes range.

The availability of the hydrogeological conceptual model facilitates the evaluation of the vulnerability and resilience of this specific CO_2-rich natural groundwater that is potentially confronted with climate change or conflicts with increasing groundwater exploitation in the area. In this sense, the large spatial (also in depth) and temporal scales involved in the occurrence of the Vilajuïga water makes it resilient to a recharge decrease due to future climatic scenarios and low vulnerability to intensive pumping occurring at distances larger than 1 km from the exploitation well. Given its heritage value as rare groundwater in the southern slope of the Eastern Pyrenees, purposeful monitoring is thus necessary to track changes, anticipate impacts, and avoid risk.

Declarations

References

Alfonso P, Melgarejo JC (2008) Valor patrimonial de las pegmatitas del Cap de Creus. IX Congreso Internacional sobre Patrimonio Geológico y Minero [Heritage value of the pegmatites of Cap de Creus. IX International Congress on Geological and Mining Heritage]. Almeria, Spain, September 2008, pp 111–118

Appelo CA, Postma D (2005) Geochemistry, groundwater and pollution, 2nd edn. Balkema, Rotterdam, The Netherlands

Ascione A, Ciotoli G, Bigi S, Buscher J, Mazzoli S, Ruggiero L, Sciarra A, Tartarello NC, Valente E (2018) Assessing mantle versus crustal sources for non-volcanic degassing along fault zones in the actively extending southern Apennines mountain belt (Italy). GSA Bull 130(9–10):1697–1722. https://doi.org/10.1130/b31869.1

Bach J (1986) Sedimentación holocena en el litoral emergido de "l'Alt Empordà" [NE de Catalunya] [Holocene sedimentation in the emerged coast of the Alt Emporda, NE Catalonia]. Acta Geol Hispánica 21–22:195–203

Barros R, Defourny A, Collignon A, Jobé P, Dassargues A, Piessens K, Welkenhuysen K (2021) A review of the geology and origin of CO2 in mineral water springs in east Belgium. Geol Belgica 24:17–31. https://doi.org/10.20341/gb.2020.023

Bense VF, Gleeson LSE, Scibek J (2013) Fault zone hydrogeology. Earth-Sci Rev 127:171–192. https://doi.org/10.1016/j.earscirev.2013.09.008

Brusi D, Menció A, Roqué C, Ramonell C, Mas-Pla J (2011) Isotopic characterization of groundwater in Western Pyrenees. In: Otero N, Soler A, Audí C eds) 9th International Symposium on Applied Isotope Geochemistry, Book of Abstracts. Tarragona, Spain, September 2011, pp 19–23

Calbó J, Conçalves M, Barrera-Escoda A, García-Serrano J, Doblas-Reyes F, Guemas V, Cunillera J, Altava V (2016) Projeccions climàtiques i escenaris de futur [Climate projections and future scenarios]. In: Martín-Vide J (ed) Tercer Informe sobre el Canvi Climàtic a Catalunya. del Consell Assessor per al Desenvolupament Sostenible i l'Institut d'Estudis Catalans, Barcelona, pp 111–133

Cartwright I, Weaver T, Tweed S, Ahearne D, Cooper M, Czapnik K, Tranter J (2002) Stable isotope geochemistry of cold CO_2-bearing mineral spring waters, Daylesford, Victoria, Australia: sources of gas and water and links with waning volcanism. Chem Geol 185(1–2):71–91. https://doi.org/10.1016/s0009-2541(01)00397-7

Carreira PM, Marques JM, Graça RC, Aires-Barros L (2008) Radiocarbon application in dating complex hot and cold CO2-rich mineral water systems: a review case studies ascribed to northern Portugal. Appl Geochem 23:2817–2828

Carreira PM, Marques JM, Carvalho MR, Nunes D, da Silva MA (2014) Carbon isotopes and geochemical processes in CO2-rich cold mineral water, N-Portugal. Environ Earth Sci 71(6):2941–2953. https://doi.org/10.1007/s12665-013-2671-x

Cerón JC, Martín-Vallejo M, García-Rossell L (2000) CO_2-rich thermomineral groundwater in the Betic Cordilleras, southeastern Spain: genesis and tectonic implications. Hydrogeol J 8(2):209–217. https://doi.org/10.1007/s100400050239

Choi BY, Yun ST, Kim KH, Choi HS, Chae GT, Lee PK (2014) Geochemical modeling of CO_2–water–rock interactions for two different hydrochemical types of CO_2-rich springs in Kangwon District, Korea. J Geochem Explor 144:49–62. https://doi.org/10.1016/j.gexplo.2014.02.009

Clark ID (2015) Groundwater, geochemistry and isotopes. CRC, Boca Raton, FL

Clark ID, Fritz P (1997) Environmental isotopes in hydrogeology. Lewis, New York

Dahlin T, Zhou B (2006) Multiple-gradient array measurements for multichannel 2D Resistivity imaging. Near Surf Geophys 4:113–123. https://doi.org/10.3997/1873-0604.2005037

Defourny A, Blard PH, Zimmermann L, Jobé P, Collignon A, Nguyen F, Dassargues A (2022) $\delta^{13}C$, $CO_2/^3He$ and $^3He/^4He$ ratios reveal the presence of mantle gas in the CO_2-rich groundwaters of the Ardennes massif (Spa, Belgium). Hydrol Earth Syst Sci 26:2637–2648. https://doi.org/10.5194/hess-26-2637-2022

Deer WA, Howie RA, Zussman J (2013) An introduction to the rock-forming minerals, 3rd edn. The Mineralogical Society, London

Do HK, Yu S, Yun ST (2020) Hydrochemical parameters to assess the evolutionary process of CO2-rich spring water: a suggestion for evaluating CO2 leakage stages in silicate rocks. Water 12(12):3421. https://doi.org/10.3390/w12123421

Domenico PA, Schwartz FW (1998) Physical and chemical hydrogeology, 2nd edn. Wiley, Chichester, UK

Evans WC, Sorey ML, Cook AC, Kennedy BM, Shuster DL, Colvard EM, Huebner MA (2002) Tracing and quantifying magmatic carbon discharge in cold groundwaters: lessons learned from Mammoth Mountain, USA. J Volcanol Geothermal Res 114(3–4):291–312. https://doi.org/10.1016/s0377-0273(01)00268-2

Fleta J, Arasa A, Escuer J (1991) El neógeno del Empordà y Baix Ebre (Catalunya) [The Neogene of the Empordà and Baix Ebre regions, Catalonia]. Acta Geol Hispànica 26:159–171

Folch A, Mas-Pla J (2008) Hydrogeological interactions between fault zones and alluvial aquifers in regional flow systems. Hydrol Process 22(17):3476–3487. https://doi.org/10.1002/hyp.6956

Foster S, Garduño H (2012) Groundwater-resource governance: are governments and stakeholders responding to the challenge? Hydrogeol J 21:317–320. https://doi.org/10.1007/s10040-012-0904-9

Gat JR (2010) Isotope hydrology: a study of the water cycle. Imperial College Press, London, 197 pp

Giggenbach WF (1988) Geothermal solute equilibria, derivation of Na–K–Mg–Ca geoindicators. Geochem Cosmochim Acta 52:2749–2765

Gilfillan SMV, Györe D, Flude S, Johnson G, Bond CE, Hicks N, Lister R, Jones DG, Kremer Y, Haszeldine RS, Stuart FM (2019) Noble gases confirm plume-related mantle degassing beneath Southern Africa. Nat Commun 10. https://doi.org/10.1038/s41467-019-12944-6

Gray M (2013) Geodiversity: valuing and conserving abiotic nature. Wiley, Chichester, UK

Han LF, Plummer LN, Aggarwal P (2012) A graphical method to evaluate predominant geochemical processes occurring in groundwater systems for radiocarbon dating. Chem Geo 318–319:88–112. https://doi.org/10.1016/j.chemgeo.2012.05.004

Hem JD (1985) Study and Interpretation of chemical characteristics of natural water, 3rd edn. USGS Water Suppl Pap 2254

IAEA (2013) Dating old groundwater. International Atomic Energy Agency, Vienna, p 376

IAEA/WMO (2021) Global network of isotopes in precipitation. The GNIP database. http://www.iaea.org/water. Accessed on June 2021

ICGC (2001) Mapa Geològic de Catalunya E 1:25.000, Full Garriguella (220-2-2) [Geological Map of Catalonia E 1:25000, Garriguella Sheet (220-2-2)]. Institut Cartogràfic i Geològic de Catalunya, Barcelona, Spain

ICGC (2013) Mapa Hidrogeològic de Catalunya E 1:25.000, Full Castelló d'Empúries (258-2-1) [Geological Map of Catalonia E 1:25000, Castelló d'Empúries Sheet (258-2-1)]. Institut Cartogràfic i Geològic de Catalunya, Barcelona, Spain

ICGC (2022) Geological maps. Institut Cartogràfic i Geològic de Catalunya. http://www.icgc.cat. Accessed Jan 2022

IDESCAT (2021) Institut d'Estadística de Catalunya (Statistical Institute of Catalonia). https://www.idescat.cat/. Accessed 29 Oct 2021

ITGE (1994a) Mapa Geológico de España E 1:50.000 "La Jonquera" [Geological map of Spain E 1:50,000 "La Jonquera"], (220). Instituto Tecnológico GeoMinero de España, Madrid

ITGE (1994b) Mapa Geológico de España E 1:50.000 "Roses" [Geological map of Spain E 1:50,000 "Roses"] (259). Instituto Tecnológico GeoMinero de España, Madrid

Karolytė R, Johnson G, Györe D, Serno S, Flude S, Stuar FM, Chivas AR, Boyce A, Gilfillan SMV (2019) Tracing the migration of mantle CO2 in gas fields and mineral water springs in south-east Australia using noble gas and stable isotopes. Geochim Cosmochim Acta 259:109–128. https://doi.org/10.1016/j.gca.2019.06.002

Kresic N, Stevanovic Z (2010) Groundwater hydrology of springs: engineering, theory, management and sustainability. Butterworth-Heinemann, Oxford, UK, p 573

LaMoreaux PE, Tanner JT (eds) (2001) Springs and bottled waters of the world: ancient history, source, occurrence, quality and use. Springer, Heidelberg, Germany, p 315

Lewis CJ, Vergés J, Marzo M (2000) High mountains in a zone of extended crust: insights into the Neogene-Quaternary topographic development of northeastern Iberia. Tectonics 19(1):86–102. https://doi.org/10.1029/1999tc900056

Loke MH, Barker RD (1996) Rapid least-squares inversion of apparent resistivity pseudosecions by a quasi-Newton method. Geophys Prospect 44(1):131–152. https://doi.org/10.1111/j.1365-2478.1996.tb00142.x

Małoszewski P, Zuber A (1982) Determining the turnover time of groundwater systems with the aid of environmental tracers. J Hydrol 57(3–4):207–231. https://doi.org/10.1016/0022-1694(82)90147-0

Marqués JM, Monteiro Santos FA, Graça RC, Castro R, Aires-Barro L, Mendez Victor LA (2001) A geochemical and geophysical approach to derive a conceptual circulation model of CO 2-rich mineral waters: a case study of Vilarelho da Raia, northern Portugal. Hydrogeol J 9(6):584–596. https://doi.org/10.1007/s10040-001-0162-8

Marques JM, Andrade M, Carreira PM, Eggenkamp HGM, Graça RC, Aires-Barros L, Antunes Da Silva M (2006) Chemical and isotopic signatures of Na/HCO3/CO2-rich geofluids, North Portugal. Geofluids 6(4):273–287. https://doi.org/10.1111/j.1468-8123.2006.00144.x

Mas-Pla J, Montaner J, Solà J (1999a) Groundwater resources and quality variations due to gravel mining in coastal streams. J Hydrol 216(3/4):197–213. https://doi.org/10.1016/S0022-1694(99)00009-8

Mas-Pla J, Bach J, Viñals E, Trilla J, Estalrich J (1999b) Salinization processes in a coastal leaky aquifer (Alt Empordà, NE Spain). Phys Chem Earth, Part B: Hydrol Oceans Atmos 24(4):337–341. https://doi.org/10.1016/S1464-1909(99)00010-6

Mas-Pla J, Menció A, Bach J, Soler D, Zamorano M, Brusi D (2016a) Trace element groundwater pollution hazard in regional hydrogeological systems (Empordà basin, NE Spain). Water Air Soil Pollut 227:218–240. https://doi.org/10.1007/s11270-016-2891-2

Mas-Pla J, Batalla RJ, Cabello A, Gallart F, Llorens P, Pascual D, Pla E, Pouget L, Termes M, Vergonyós L (2016b) Recursos hidrològics [Water resources]. In: Martín-Vide J (ed) Tercer Informe sobre el Canvi Climàtic a Catalunya. Consell Assessor per al Desenvolupament Sostenible and Institut d'Estudis Catalans, Barcelona, pp 161–187

Masanés C (2021) Vilajuïga, l'aigua [Vilajuïga, and its water]. Gavarres, Girona, Spain, 132 pp

Matyasik I, Spunda K, Kania M, Wencal K (2018) Genesis of hydrogen sulfide in carbonate reservoirs. NAFTA-Gaz 74(9):627–635. https://doi.org/10.18668/NG.2018.09.01

MedECC (2020) Climate and environmental change in the Mediterranean Basin: current situation and risks for the future. First Mediterranean Assessment Report. Cramer W, Guiot J, Marini K (eds) Union for the Mediterranean, Plan Bleu, UNEP/MAP, Marseille, France, 632 pp

Montaner J (2010) El flux hidrogeològic de la plana litoral del Baix Ter. Evolució fluvial, caracterització hidrològica i pautes de gestió [Hydrogeological Flow at the Baix Ter alluvial plain: fluvial evolution, hydrological characterization and management approaches], vol 2. Càtedra d'Ecosistemes Litorals Mediterranis, Museu de la Mediterrània, Col. Recerca i Territori, Girona, Spain, 236 pp

Parkhurs DL, Appelo CAJ (2013) Description of input and examples for PHREEQC version 3: a computer program for speciation, batch-reaction, one-dimensional transport, and inverse geochemical calculations. US Geol Survey Techn Methods Book 6, A43, p 497. https://doi.org/10.3133/tm6A43

Pauwels H, Fouillac C, Goff F, Vuataz FD (1997) The isotopic and chemical composition of CO2-rich thermal waters in the Mont-Dore region (Massif-Central, France). Appl Geochem 12(4):411–427. https://doi.org/10.1016/s0883-2927(97)00010-3

Pearson FJ (1965) Use of C-13/C-12 ratios to correct radiocarbon ages of material initially diluted by limestone. In Proceedings of the 6th International Conference on Radiocarbon and Tritium Dating, Pullman, WA, June 1965, 357 pp

Pearson FJ, Hanshaw BB (1970) Sources of dissolved carbonate species in groundwater and their effects on carbon-14 dating. In: Isotope Hydrology 1970, IAEA Symposium 129, Vienna, March 1970, pp 271–286

Pujadas J, Casas JM, Muñoz JA, Sàbat F (1989) Thrust tectonics and Paleogene syntectonic sedimentation in the Empordà area, southeastern Pyrenees. Geodinam Acta 3(3):195–206

Railsback LB (1993) A geochemical view of weathering and the origin of sedimentary rocks and natural waters. J Geol Edu 41(5):404–411. https://doi.org/10.5408/0022-1368-41.5.404

Rodak C, Silliman SE, Bolster D (2013) Time-dependent health risk from contaminated groundwater including use of reliability, resilience, and vulnerability as measures. J Am Water Resour Assoc 50(1):14–28. https://doi.org/10.1111/jawr.12103

Romano P, Liotta M (2020) Using and abusing Giggenbach ternary Na-K-Mg diagram. Chem Geol 541:119577. https://doi.org/10.1016/j.chemgeo.2020.119577

Roqué C, Pallí L (1994) Geologia del massís de les Gavarres [Geology of the Gavarres Massif]. Estudis sobre el Baix Empordà 13:5–98

Saula E, Picart J, Mató E, Llenas M, Losantos M, Beràstegui X, Agustí J (1996) Evolución geodinámica de las fosas del Empordà y Sierras Transversales [Geodynamic evolution of the Empordà basin and the Transveral Range]. Acta Geol Hispánica 29:55–75

Schofield S, Jankowski J (2004) Hydrochemistry and isotopic composition of Na–HCO3-rich groundwaters from the Ballimore region, central New South Wales, Australia. Chem Geol 211(1–2):111–134. https://doi.org/10.1016/j.chemgeo.2004.06.026

Soler D, Zamorano M, Roqué C, Menció A, Boy M, Bach J, Brusi D, Mas-Pla J (2014) Evaluación de la influencia de las estructuras tectónicas en la recarga del sistema hidrogeológico de la depresión del Alt Empordà (NE España) en base a datos hidroquímicos e isotópicos [Evaluation of the influence of tectonic structures in the hydrogeological recharge of the Alt Empordà basin (NE Spain) base don hydrochemical and isotopic data]. In: Gómez-Hernández JJ, Rodrigo-Ilarri J (eds) II Congreso Ibérico de las Aguas Subterráneas. Universitat Politècnica de València, Spain, pp 853–872

Tweed SO, Weaver TR, Cartwright I (2004) Distinguishing groundwater flow paths in different fractured-rock aquifers using groundwater chemistry: Dandenong Ranges, southeast Australia. Hydrogeol J 13(5–6):771–786. https://doi.org/10.1007/s10040-004-0348-y

Vilà M, Pin C, Liesa M, Enrique P (2007) LPHT metamorphism in a late orogenic transpressional setting, Albera Massif, NE Iberia: implications for the geodynamic evolution of the Variscan Pyrenees. J Metamorphic Geol 25(3):321–347. https://doi.org/10.1111/j.1525-1314.2007.00698.x